

High-SNR Comparison of Linear Precoding and DPC in RIS-Aided MIMO Broadcast Channels

Dominik Semmler, Benedikt Fesl, Michael Joham, and Wolfgang Utschick

School of Computation, Information and Technology, Technical University of Munich, Germany

email: {dominik.semmler,benedikt.fesl,joham,utschick}@tum.de

Abstract—We compare dirty paper coding (DPC) and linear precoding methods in a reconfigurable intelligent surface (RIS)-aided high-signal-to-noise ratio (SNR) scenario, where the channel between the base station (BS) and the RIS is dominated by a line-of-sight (LOS) component. Furthermore, we consider two groups of users where one group can be efficiently served by the BS, whereas the other one has a negligible direct channel and has to be served via the RIS. Within this scenario, we analytically show fundamental differences between DPC and linear methods. In particular, our analysis addresses two essential aspects, i.e., the orthogonality of the BS-RIS channel with the direct channel and a channel mitigation term, depending on the number of RIS elements, that is present only for linear precoding techniques. The mitigation term generally leads to strong limitations for the linear method, especially for random or statistical phase shifts. Moreover, we discuss under which circumstances this mitigation term is negligible and in which scenarios DPC and linear precoding lead to the same performance.

Index Terms—DPC, zero-forcing, LOS, exponential integral

I. INTRODUCTION

RISs are considered to be an important technology for future wireless communication systems which are able to significantly enhance the system performance [1]. The RIS is a surface consisting of many passive elements which allow to reconfigure the channel environment. Modelling the RIS is still under ongoing research. Various architectures for RISs exist, e.g., simultaneously transmitting and reflecting (STAR) RISs (see [2], [3]), beyond diagonal (BD)-RISs where the reflecting elements are connected to each other (see [4], [5]), as well as active RISs (see [6], [7]). The conventional architecture is the passive, single-connected RIS, where the elements are not connected with each other. This architecture is usually modeled with the phase shift model for which a considerable amount of literature is available (see, e.g., [1], [8]–[12]). Models based on the impedance and scattering formulations (see [4], [13]) have been compared to the conventional phase-shift model in [14]–[17]. These models also allow to incorporate mutual coupling (see [13], [18], [19]) between the reflecting elements in the system model. Mutual coupling can, however, also be taken into account with decoupling networks (see [19]) which have the beneficial aspect that the resulting system model has the same structure as in the case without mutual coupling. Throughout this article, we only consider the conventional phase shift model without mutual coupling. However, the results of this article can be directly extended to the model in [14] as well as to mutual coupling with the help of decoupling networks (see [19]).

A major challenge for the RIS design is the large number of reflecting elements which have to be jointly optimized with the transmit filters in a downlink scenario. The classical approach is to first estimate the channel and, afterwards, solve the joint optimization of precoders and reflecting elements. When considering perfect estimates, and, hence, assuming perfect instantaneous channel state information (CSI), the RIS already showed a significant performance increase in various scenarios, e.g., for power consumption [1], energy efficiency [8], as well as for spectral efficiency [9]–[11]. However, channel estimation in a RIS scenario (see [20], [21]) is difficult due to the high number of parameters. While there are methods which approach this problem (see [22], [23]), designing the reflecting elements only based on the statistics of the channel (see [12], [24]–[26]) circumvents the channel estimation phase. Using only statistical CSI does not require updating the reflecting elements in each coherence interval of the channel which is an additional upside. In this article, we mathematically analyze the spectral efficiency (SE) when the reflecting elements are optimized based on instantaneous CSI, statistical CSI as well as when they are chosen randomly.

When it comes to the precoder design at the base station, we consider both DPC (see [27], [28]) as well as linear approaches. For the linear methods, we use zero-forcing beamforming which is high-SNR optimal. DPC has already been compared to zero-forcing in the conventional channel model without the RIS (see [29], [30]). DPC, being the optimal choice for the downlink scenario, always leads to a better SE which is especially noticeable when the channel is ill-conditioned. In this article, the difference between DPC and linear precoding is analyzed mathematically and we show that their difference is generally significant when including an RIS.

An important aspect throughout this article is that we are considering a scenario in which the channel between the BS and the RIS is given by a rank-one matrix, motivated by the fact that the BS and the RIS are typically deployed in LOS and, additionally, at a considerable height (see [31]). This has already been assumed in a number of articles (see, e.g., [32]–[36]). Under this assumption, the eigenvalue result of [37] holds, i.e., the eigenvalues of the composite channel Gram matrix (we assume that all user channels are stacked into this matrix), including the RIS, can, at maximum, be improved to the next larger eigenvalues of the composite direct channel Gram matrix. While this result shows clear limitations, the RIS can still have a significant impact on the scenario (see [38]), especially for a lower number of users.

Furthermore, we consider a scenario where the users can be divided into two groups. One group consists of users with a strong direct channel, which could be efficiently served by the BS without the RIS, whereas the other group consists of users with a negligible direct channel and have to be served via the RIS. In this case, the eigenvalues of the weak users' direct channels can be modeled as being approximately zero, and, according to [37], only one eigenvalue can be improved due to the rank-one assumption for the BS-RIS channel. Therefore, only one user of the weak user group will be additionally served. Accordingly, throughout this article, we assume w.l.o.g. that the number of weak users to be served via the RIS is one.

If the strong users did not exist and only the weak users were present, the direct composite Gram channel matrix has only one non-zero eigenvalue and would be rank-one. Consequently, the optimal solution for sum-SE maximization is to only allocate one user in total. This scenario was already analyzed in [32] under the max-min fairness criterion in an asymptotic regime, where it was also proposed to only serve a single user. In contrast, when strong users do exist and the direct channel is non-negligible, the situation is different and it is not necessarily sum-SE optimal to just improve the weak user's channel gain as the additional strong users introduce interference.

In this article, this scenario, with some direct channels being non-negligible, is analyzed in the high-SNR regime. For high SNR values, all the strong direct channel users are allocated as well as one additional user of the weak users group via the RIS. Hence, we obtain a rank-improvement scenario for which the RIS is particularly suited (see [39]).

In particular, we make the following contributions:

- We derive the optimal SE expressions for linear precoding and DPC in the high-SNR regime. These expressions allow us to analyze this scenario mathematically. Additionally, we can show that fundamental differences between DPC and linear precoding occur also in a RIS-assisted scenario.
- We show analytically that linear precoding suffers from a mitigation term that completely vanishes in the case of DPC. Moreover, we show the importance of the BS-RIS channel being orthogonal to the direct channel and that DPC has an advantage if this condition is not perfectly fulfilled.
- More results are derived from the considerations above. Firstly, only for DPC, it is high-SNR optimal to maximize the weak user's channel gain, whereas for linear precoding, the solution is more intricate and has no closed-form. Secondly, when considering random or statistical phase shifts, the SE for linear precoding saturates for an increasing number of RIS elements in case of i.i.d. Rayleigh fading, whereas for DPC, the SE is increasing monotonically.

II. SYSTEM MODEL

A downlink (DL) scenario is considered in which $K + 1$ single-antenna users are served by a single BS having N_B an-

tennas. Additionally, we assume one RIS having N_R reflecting elements. The channel from the BS to the k -th user reads as

$$\mathbf{h}_k^H = \mathbf{h}_{d,k}^H + \mathbf{h}_{r,k}^H \Theta \mathbf{G} \in \mathbb{C}^{1 \times N_B} \quad (1)$$

where $\mathbf{h}_{d,k}^H \in \mathbb{C}^{1 \times N_B}$ is the direct channel from the BS to the k -th user, $\mathbf{h}_{r,k}^H \in \mathbb{C}^{1 \times N_R}$ is the reflecting channel from the RIS to the k -th user, and

$$\mathbf{G} = \sqrt{L_G N_B} \mathbf{a} \mathbf{b}^H \in \mathbb{C}^{N_R \times N_B} \quad (2)$$

is the LOS rank-one channel from the BS to the RIS where L_G is the pathloss. We have a scaling with N_B as the steering vector \mathbf{b} is normalized such that $\|\mathbf{b}\|_2 = 1$, whereas $\|\mathbf{a}\|_2^2 = N_R$. The matrix $\Theta = \text{diag}(\boldsymbol{\theta}) \in \mathbb{C}^{N_R \times N_R}$ with $\boldsymbol{\theta} \in \{z \in \mathbb{C}^{N_R} : z_n = e^{j\phi_n}, \phi_n \in [0, 2\pi), \forall n\}$ is the phase manipulation at the RIS. Recently, new models appeared based on the impedance formulation (see [14]) where the constraints are of the form $\{z \in \mathbb{C}^{N_R} : z_n = e^{j\phi_n} - 1, \phi_n \in [0, 2\pi), \forall n\}$. While we consider the unit-modulus constraint set from above, all the results from this article can be directly transferred to the other models. Additionally, we neglect mutual coupling in this article and, hence, the phase shift matrix is diagonal. However, when using decoupling networks (see [19]), the results can be directly extended to the case of mutual coupling as the phase shift matrix becomes diagonal again in this case. Even for non-diagonal Θ matrices, e.g., in case of mutual coupling without decoupling networks, or in the case of BD-RISs, similar expressions as in this article can be obtained.

In case Θ is diagonal, a more compact notation is available and is used for notational convenience throughout this article. In particular, we rewrite \mathbf{h}_k^H as

$$\mathbf{h}_k^H = \mathbf{h}_{d,k}^H + \mathbf{h}_{c,k}^H \boldsymbol{\theta} \mathbf{b}^H \in \mathbb{C}^{1 \times N_B} \quad (3)$$

with the cascaded channel being defined as

$$\mathbf{h}_{c,k}^H = \mathbf{h}_{r,k}^H \text{diag}(\mathbf{a}) \sqrt{L_G N_B}. \quad (4)$$

As pointed out in the introduction, we assume that exactly one of the users has a negligible direct channel and that this user can only be properly served via the RIS. We consider user $K + 1$ to be this weak user, whereas the other, i.e., strong users (1 until K) are stacked into the channel matrices $\mathbf{H}_d^s = [\mathbf{h}_{d,1}, \dots, \mathbf{h}_{d,K}]^H$, $\mathbf{H}_r^s = [\mathbf{h}_{r,1}, \dots, \mathbf{h}_{r,K}]^H$ and according to the notation in (3) equivalently $\mathbf{H}_c^s = [\mathbf{h}_{c,1}, \dots, \mathbf{h}_{c,K}]^H$. Assuming that only one user has a negligible direct channel is motivated by the fact that when having a group of weak users with no direct channel, only one can be additionally allocated via the RIS. This is because the BS-RIS channel is rank-one and this fact has been discussed in the introduction based on the eigenvalue result of [37]. However, this can also be directly observed when considering the composite channel matrix

$$\mathbf{H} = \begin{bmatrix} \mathbf{H}_d^s \\ \mathbf{0} \end{bmatrix} + \mathbf{H}_c \boldsymbol{\theta} \mathbf{b}^H \quad (5)$$

where \mathbf{H}_c are the stacked cascaded channels of all users. We can directly see that the maximum rank of the composite channel matrix is $\text{rank}(\mathbf{H}) \leq \text{rank}(\mathbf{H}_d^s) + 1 = K + 1$ and,

therefore, maximally one additional user is allocated. Hence, w.l.o.g we can write the composite channel matrix as

$$\mathbf{H} = \begin{bmatrix} \mathbf{H}^s \\ \mathbf{h}_{K+1}^H \end{bmatrix} = \underbrace{\begin{bmatrix} \mathbf{H}_d^s \\ \mathbf{0}^H \end{bmatrix}}_{\mathbf{H}_d} + \underbrace{\begin{bmatrix} \mathbf{H}_c^s \\ \mathbf{h}_{c,K+1}^H \end{bmatrix}}_{\mathbf{H}_c} \boldsymbol{\theta} \mathbf{b}^H \in \mathbb{C}^{K+1 \times N_B}. \quad (6)$$

III. SE EXPRESSIONS FOR DPC AND ZF

In this section, we derive the asymptotic SE expressions at high-SNR for both linear precoding and DPC. To this end, we exploit the rank-one property of the BS-RIS channel. Firstly, we split the channel matrix \mathbf{H} in the subspace via the BS-RIS channel $\mathbf{b}\mathbf{b}^H$ and its orthogonal space \mathbf{P}_b^\perp as

$$\mathbf{H} = \mathbf{H}_d \mathbf{P}_b^\perp + (\mathbf{H}_c \boldsymbol{\theta} + \mathbf{H}_d \mathbf{b}) \mathbf{b}^H \quad (7)$$

where \mathbf{P}_b^\perp is the orthogonal projector

$$\mathbf{P}_b^\perp = \mathbf{I} - \mathbf{b}\mathbf{b}^H. \quad (8)$$

Similar to [37], this allows us to express the channel Gram matrix as

$$\mathbf{H}\mathbf{H}^H = \begin{bmatrix} \mathbf{C}_s & \mathbf{0} \\ \mathbf{0}^T & 0 \end{bmatrix} + \mathbf{D}\bar{\boldsymbol{\theta}}\bar{\boldsymbol{\theta}}^H\mathbf{D}^H \quad (9)$$

with the definitions

$$\mathbf{C}_s = \mathbf{H}_d^s \mathbf{P}_b^\perp \mathbf{H}_d^{s,H} \in \mathbb{C}^{K \times K}, \quad (10)$$

$$\mathbf{D} = [\mathbf{H}_c, \mathbf{H}_d \mathbf{b}], \quad \bar{\boldsymbol{\theta}} = [\boldsymbol{\theta}^H \quad 1]^H. \quad (11)$$

The matrix \mathbf{C}_s corresponds to the direct Gram channel matrix excluding the direction \mathbf{b} to the RIS, whereas $\mathbf{D}\bar{\boldsymbol{\theta}}$ represents the channel via the direction \mathbf{b} , i.e., the direction via the RIS. Note, that also the direct channel component $\mathbf{H}_d \mathbf{b}$ is incorporated in the part $\mathbf{D}\bar{\boldsymbol{\theta}}$. In the following, we assume that $\mathbf{e}_{K+1}^T \mathbf{D}\bar{\boldsymbol{\theta}} = \mathbf{h}_{c,K+1}^H \boldsymbol{\theta} \neq 0$ where \mathbf{e}_n is the n -th canonical basis vector. This means that the weak user $K+1$ has a non-zero RIS-user channel. For example, in case no RIS were present, i.e., $\boldsymbol{\theta} = \mathbf{0}$, the weak user would effectively not exist.

A. Linear Precoding

For linear precoding, it is known that zero-forcing is optimal at high-SNR and the sum-SE is given by (see [30])

$$\text{SE}_{\text{ZF-General}} = \sum_{k=1}^K \log_2 \left(1 + \frac{\gamma_k}{\mathbf{e}_k^T (\mathbf{H}\mathbf{H}^H)^{-1} \mathbf{e}_k} \right) \quad (12)$$

where γ_k are the power allocations. Under the condition $\mathbf{h}_{c,K+1}^H \boldsymbol{\theta} \neq 0$ and by defining

$$\mathbf{D}_s = [\mathbf{H}_c^s, \mathbf{H}_d^s \mathbf{b}] \quad (13)$$

as the channel component via the direction \mathbf{b} of only the strong users, the inverted channel gain for the k -th user can be written (see Appendix A) as

$$\mathbf{e}_k^T (\mathbf{H}\mathbf{H}^H)^{-1} \mathbf{e}_k = \begin{cases} \mathbf{e}_k^T \mathbf{C}_s^{-1} \mathbf{e}_k & \text{if } k \leq K \\ \frac{1 + \bar{\boldsymbol{\theta}}^H \mathbf{D}_s^H \mathbf{C}_s^{-1} \mathbf{D}_s \bar{\boldsymbol{\theta}}}{|\mathbf{h}_{c,K+1}^H \boldsymbol{\theta}|^2} & \text{if } k = K + 1. \end{cases} \quad (14)$$

Considering a uniform power allocation $\gamma_k = \frac{P_{\text{Tx}}}{K} = \bar{p}$, which is high-SNR optimal, we obtain the sum-SE

$$\text{SE}_{\text{ZF}} = \sum_{k=1}^K \log_2 \left(1 + \frac{\bar{p}}{\mathbf{e}_k^T \mathbf{C}_s^{-1} \mathbf{e}_k} \right) + \log_2 \left(1 + \frac{\bar{p} |\mathbf{h}_{c,K+1}^H \boldsymbol{\theta}|^2}{1 + \bar{\boldsymbol{\theta}}^H \mathbf{D}_s^H \mathbf{C}_s^{-1} \mathbf{D}_s \bar{\boldsymbol{\theta}}} \right). \quad (15)$$

B. DPC

For DPC, we use the dual-uplink (UL) representation

$$\text{SE}_{\text{DPC-General}} = \log_2 \det (\mathbf{I} + \mathbf{H}^H \mathbf{Q} \mathbf{H}) \quad (16)$$

where choosing the transmit covariance matrix $\mathbf{Q} = \mathbf{I} \frac{P_{\text{Tx}}}{K} = \bar{\mathbf{I}} \bar{p}$ is high-SNR optimal. Defining λ_k as the eigenvalues of \mathbf{C}_s in decreasing order with the corresponding eigenvectors \mathbf{u}_k , the sum-SE for DPC is given (see Appendix B) by

$$\text{SE}_{\text{DPC}} = \sum_{k=1}^K \log_2 (1 + \lambda_k \bar{p}) + \log_2 \left(1 + |\mathbf{h}_{c,K+1}^H \boldsymbol{\theta}|^2 \bar{p} + \sum_{k=1}^K |\bar{\boldsymbol{\theta}}^H \mathbf{D}^H \mathbf{u}_k|^2 \frac{\bar{p}}{1 + \lambda_k \bar{p}} \right). \quad (17)$$

Having derived the sum-SE expressions for linear precoding and DPC in (15) and (17), we will now analyze the implications arising from these two formulations. It is important to note that both expressions are optimal in the high-SNR regime.

IV. HIGH-SNR ANALYSIS OF DPC AND LINEAR PRECODING

In the following, we are considering the high-SNR regime (for which (15) and (17) are optimal). Hence, we have $\bar{p} \rightarrow \infty$ and obtain the asymptotic expressions of (15) and (17)

$$\overline{\text{SE}}_{\text{Lin}} = \underbrace{\sum_{k=1}^K \log_2 \left(\frac{\bar{p}}{\mathbf{e}_k^T \mathbf{C}_s^{-1} \mathbf{e}_k} \right)}_{\overline{\text{SE}}_{\text{Lin,d}}} + \underbrace{\log_2 \left(\frac{|\mathbf{h}_{c,K+1}^H \boldsymbol{\theta}|^2 \bar{p}}{1 + \bar{\boldsymbol{\theta}}^H \mathbf{D}_s^H \mathbf{C}_s^{-1} \mathbf{D}_s \bar{\boldsymbol{\theta}}} \right)}_{\overline{\text{SE}}_{\text{Lin,r}}}, \quad (18)$$

$$\overline{\text{SE}}_{\text{DPC}} = \underbrace{\log_2 \det (\mathbf{C}_s \bar{p})}_{\overline{\text{SE}}_{\text{DPC,d}}} + \underbrace{\log_2 \left(|\mathbf{h}_{c,K+1}^H \boldsymbol{\theta}|^2 \bar{p} \right)}_{\overline{\text{SE}}_{\text{DPC,r}}} \quad (19)$$

for linear precoding and DPC, respectively. DPC is the capacity achieving method, and after a reformulation of (19), an important observation can be made.

Proposition 1. *In the high-SNR regime, the SE of DPC can be given as*

$$\overline{\text{SE}}_{\text{DPC}} = \log_2 \det (\mathbf{H}_d^s \mathbf{H}_d^{s,H} \bar{p}) + \log_2 (\mathbf{b}^H \mathbf{P}_{\mathbf{H}^H}^\perp \mathbf{b}) + \log_2 (|\mathbf{h}_{c,K+1}^H \boldsymbol{\theta}|^2 \bar{p}). \quad (20)$$

Proof. This result can be directly obtained from (19) by rewriting $\log_2 \det (\mathbf{C}_s) = \log_2 \det (\mathbf{H}_d^s \mathbf{H}_d^{s,H} - \mathbf{H}_d^s \mathbf{b}\mathbf{b}^H \mathbf{H}_d^{s,H}) = \log_2 \det (\mathbf{H}_d^s \mathbf{H}_d^{s,H}) + \log_2 (1 - \mathbf{b}^H \mathbf{H}_d^{s,H} (\mathbf{H}_d^s \mathbf{H}_d^{s,H})^{-1} \mathbf{H}_d^s \mathbf{b})$. \square

This reformulation is important as the expression matches the intuition in the sense that the users with non-negligible direct channels are served via the BS corresponding to the term

$\log_2 \det(\mathbf{H}_d^s \mathbf{H}_d^{s,H} \bar{p})$. Furthermore, when including the RIS, one additional user with negligible direct channel is served via the RIS corresponding to the term $\log_2(|\mathbf{h}_{c,K+1}^H \boldsymbol{\theta}|^2 \bar{p})$. However, we further have the term $\log_2(\mathbf{b}^H \mathbf{P}_b^\perp \mathbf{b})$, which highlights the importance of the BS-RIS channel being orthogonal to the direct channels. This is an important observation which is analyzed in more detail in Section IV-A.

The SE for linear precoding leads to a fundamentally different structure. However, we can see that the expression in (18) still has a special structure in the sense that the strong users $k = 1, \dots, K$ do not depend on the reflecting elements which will be discussed in the following.

It is known that zero-forcing precoding is optimal in the high-SNR regime. Hence, the interference has to be completely cancelled by precoding at the BS. Considering user $K+1$, the corresponding channel is given by $\mathbf{h}_{K+1} = \mathbf{h}_{c,K+1}^H \boldsymbol{\theta} \mathbf{b}^H \in \mathbb{C}^{1 \times N_B}$ as this user has no direct channel. To achieve interference cancellation, all precoders of the strong users $1, 2, \dots, K$ have to be orthogonal to the channel \mathbf{h}_{K+1} , i.e., the direction \mathbf{b} via the RIS. Hence, the strong users are spatially separated and we obtain the structure in (18) as all precoders for the users $1, 2, \dots, K$ are chosen orthogonal to the channel via the RIS. From this spatial separation, it additionally follows that the channel part via the direction \mathbf{b} , i.e., $\mathbf{H}_d^s \mathbf{b} \mathbf{b}^H$ and $\mathbf{H}_c^s \boldsymbol{\theta} \mathbf{b}^H$, is decremental for the strong users. This is taken care of by the precoder of user $K+1$ and the negative impact is expressed in the channel mitigation term $\bar{\boldsymbol{\theta}}^H \mathbf{D}_s^H \mathbf{C}_s^{-1} \mathbf{D}_s \bar{\boldsymbol{\theta}}$. This problem does not arise for DPC as it can additionally cancel the interference by coding. The scenario is graphically illustrated in Fig. 1. Please note that the figure is a theoretical illustration according to the notation of (3) and the physical channel from the BS to the RIS is the $N_R \times N_B$ dimensional channel \mathbf{G} and not the direction $\mathbf{b}^H \in \mathbb{C}^{1 \times N_B}$.

Hence, fundamental differences between DPC and linear precoding arise which are stated in the following theorem.

Theorem 1. *In the high-SNR regime, the difference between DPC and linear precoding can be given by*

$$\Delta \bar{SE} = \bar{SE}_{DPC} - \bar{SE}_{Lin} \quad (21)$$

which can be further written as

$$\Delta \bar{SE} = \underbrace{\bar{SE}_{DPC,d} - \bar{SE}_{Lin,d}}_{\Delta \bar{SE}_d} + \underbrace{\bar{SE}_{DPC,r} - \bar{SE}_{Lin,r}}_{\Delta \bar{SE}_r} \quad (22)$$

with the expressions

$$\Delta \bar{SE}_d = \log_2 \det(\mathbf{C}_s) - \sum_{k=1}^K \log_2((\mathbf{e}_k^T \mathbf{C}_s^{-1} \mathbf{e}_k)^{-1}), \quad (23)$$

$$\Delta \bar{SE}_r = \log_2(1 + \bar{\boldsymbol{\theta}}^H \mathbf{D}_s^H \mathbf{C}_s^{-1} \mathbf{D}_s \bar{\boldsymbol{\theta}}). \quad (24)$$

The discussion of this theorem is separated into Section IV-A for (23) and into Section IV-B2 for (24).

A. Orthogonality of \mathbf{G} with the strong users' direct channels

We start by analyzing $\bar{SE}_{DPC,d}$ and $\bar{SE}_{Lin,d}$ which are not depending on the phases $\boldsymbol{\theta}$. Interestingly, these are exactly the

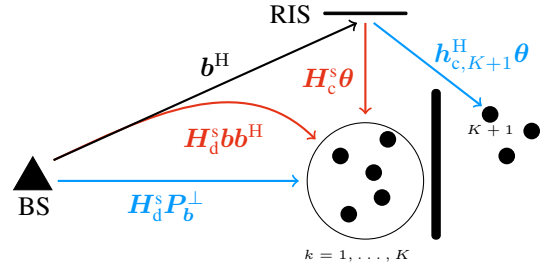


Figure 1. High-SNR scenario for ZF. In case of DPC, $\mathbf{H}_c^s \boldsymbol{\theta} \mathbf{b}^H$ and $\mathbf{H}_d^s \mathbf{b} \mathbf{b}^H$ are cancelled by coding.

asymptotic expressions for DPC and zero-forcing for a conventional system without the RIS ([29], [30]) and the term $\Delta \bar{SE}_d$ in (23) is exactly the corresponding high-SNR offset (see [30, eq. (9)]). The only difference to the conventional system in the expressions above is that instead of the Gram channel matrix $\mathbf{H}_d^s \mathbf{H}_d^{s,H}$, we have the matrix $\mathbf{C}_s = \mathbf{H}_d^s \mathbf{P}_b^\perp \mathbf{H}_d^{s,H}$. Hence, the direction \mathbf{b} , corresponding to the BS-RIS channel, is excluded. Excluding this direction is a major difference and deteriorates the performance. Also, in this case, DPC has the typical advantage over linear precoding in the sense that

$$\bar{SE}_{DPC,d} \geq \bar{SE}_{Lin,d} \quad (25)$$

holds with equality if \mathbf{C}_s is diagonal (see, e.g., [30]). However, in comparison to the conventional case, for \mathbf{C}_s to be diagonal, not only the strong users' direct channels have to be mutually orthogonal but they also have to be orthogonal to \mathbf{b} .

For example, if \mathbf{b} were orthogonal to the strong direct channels, i.e., $\mathbf{b} \in \text{null}(\mathbf{H}_d^s)$, the orthogonal projector completely vanishes and we have $\mathbf{C}_s = \mathbf{H}_d^s \mathbf{H}_d^{s,H}$. Therefore, we arrive at the conventional asymptotic expression and the negative impact of \mathbf{P}_b^\perp completely vanishes which is clearly a best-case scenario.

On the contrary, in case the direction \mathbf{b} (the BS-RIS channel) would lie within the space spanned by the strong channels, i.e., $\mathbf{b} \in \text{range}(\mathbf{H}_d^s)$, we have a worst-case scenario in which an eigenvalue of $\mathbf{H}_d^s \mathbf{P}_b^\perp \mathbf{H}_d^{s,H}$ completely vanishes. To see this, we rewrite the matrix \mathbf{C}_s as

$$\mathbf{C}_s = \mathbf{U}_s \boldsymbol{\Sigma}_s (\mathbf{I} - \mathbf{V}_s^H \mathbf{b} \mathbf{b}^H \mathbf{V}_s) \boldsymbol{\Sigma}_s \mathbf{U}_s^H \quad (26)$$

where we use the singular value decomposition (SVD) $\mathbf{H}_d^s = \mathbf{U}_s \boldsymbol{\Sigma}_s \mathbf{V}_s^H$. Because $\mathbf{b} \in \text{range}(\mathbf{H}_d^s)$, we have $\mathbf{V}_s \mathbf{V}_s^H \mathbf{b} = \mathbf{b}$ and, therefore, $\mathbf{b}^H \mathbf{V}_s \mathbf{V}_s^H \mathbf{b} = 1$. It follows that $\|\mathbf{V}_s \mathbf{b}\|_2 = 1$ and $\mathbf{P}_{\mathbf{V}_s \mathbf{b}}^\perp = \mathbf{I} - \mathbf{V}_s \mathbf{b} \mathbf{b}^H \mathbf{V}_s^H \in \mathbb{C}^{K \times K}$ is another orthogonal projector. However, this time, the projector $\mathbf{P}_{\mathbf{V}_s \mathbf{b}}^\perp$ is $K \times K$ instead of $N_B \times N_B$ and one singular value of the strong users is completely canceled. A complete stream is missing in this case and the transmission is clearly deteriorated. In a practical scenario, the orthogonality highly depends on the ratio of base station antennas N_B to the number of users with non-negligible direct channel K . In case $N_B \approx K+1$, the performance will be clearly degraded in comparison to $N_B \gg K+1$, where the channels are likely to be close to orthogonal. In summary, the orthogonality of the BS-RIS channel with the strong users' direct channels is important for the performance in a RIS-

aided scenario and is a necessary condition for DPC and linear precoding to perform equally.

B. Channel Mitigation

We focus now on the expressions $\overline{\text{SE}}_{\text{DPC},r}$ and $\overline{\text{SE}}_{\text{Lin},r}$ which contain the phase manipulations at the RIS. Interestingly, DPC and linear precoding have the same expressions with the major difference that the channel mitigation term $\bar{\boldsymbol{\theta}}^H \mathbf{D}_s^H \mathbf{C}_s^{-1} \mathbf{D}_s \bar{\boldsymbol{\theta}}$ completely disappears in case of DPC, resulting in $\Delta \overline{\text{SE}}_r$ in (24). This is an important observation, meaning that improving the weak user's channel gain is only optimal in the case of DPC; for linear precoding, a more sophisticated solution has to be constructed which takes into account the dependence of the other users.

1) *Influence of the Direct Channels:* From the mitigation term we can see that not only the channel from the RIS to the strong users $\mathbf{H}_c^s \boldsymbol{\theta}$ but the sum together with the direct channel component $\mathbf{H}_d^s \mathbf{b}$ has a negative impact on the system performance. This is important as this means that even when the strong users are significantly separated from the weak user, the mitigation term is still non-zero and we would experience a performance drop in $\overline{\text{SE}}_{\text{Lin},r}$. For example, if the reflecting channels within the mitigation term could be completely neglected (this refers to $\mathbf{H}_c^s \boldsymbol{\theta} = \mathbf{0}$) and, hence, the RIS had only impact on the user $K+1$, the mitigation term is still non-zero and reads as

$$1 + \bar{\boldsymbol{\theta}}^H \mathbf{D}_s^H \mathbf{C}_s^{-1} \mathbf{D}_s \bar{\boldsymbol{\theta}} = \frac{1}{\bar{\mathbf{b}}^H \mathbf{P}_{\mathbf{H}_d^s}^\perp \bar{\mathbf{b}}} \quad (27)$$

which can be shown by the matrix inversion lemma. Hence, if the BS-RIS channel is not orthogonal to the direct channel, the mitigation given in (27) could take any positive value and the performance is deteriorated for linear precoding. The impact of the reflecting channels can in this regard be actually beneficial as $\mathbf{H}_c^s \boldsymbol{\theta}$ could compensate to an extent for $\mathbf{H}_d^s \mathbf{b}$.

2) *Influence of the Reflecting Channels:* The drawback of linear precoding will be analyzed more deeply in the following based on the dependence of the reflecting elements. This drawback is especially pronounced in the case where $\boldsymbol{\theta}$ is chosen independently of the mitigation term in the denominator (this holds for the important cases when only the numerator, i.e., the weak user, is maximized or statistical/random phases are considered). The focus is on this scenario where the advantage of DPC is especially pronounced. We can directly bound the SE of linear precoding by dropping the mitigation term as

$$\overline{\text{SE}}_{\text{Lin},r} \leq \log_2 \left(\left| \mathbf{h}_{c,K+1}^H \boldsymbol{\theta} \right|^2 \bar{p} \right) = \overline{\text{SE}}_{\text{DPC},r} \quad (28)$$

and, hence, also for this part, DPC is always leading to a higher rate than linear precoding. This bound is of course only tight when the mitigation term is negligible in which the two schemes perform similarly. However, when the mitigation does play a role (which happens, e.g., in the important case where $N_R \rightarrow \infty$), a tighter bound has to be derived. In order to derive a new bound, we first establish the following lemma for the exponential integral.

Lemma 1. For $x > 0$, the exponential integral $E_1(x)$ can be lower bounded by

$$E_1(x)e^x > \ln \left(1 + \frac{e^{-\gamma}}{x} \right), \quad \forall x > 0. \quad (29)$$

Proof. See Appendix C. \square

Using Lemma 1, we can state the following upper bound.

Theorem 2. Under the assumption of Rayleigh fading for the reflective channels $\mathbf{h}_{r,k} \sim \mathcal{N}_{\mathbb{C}}(\mathbf{0}, \mathbf{R}_{r,k})$ $k \leq K$, expression $\mathbb{E}[\overline{\text{SE}}_{\text{Lin},r}]$ from (18) can be upper bounded as

$$\mathbb{E}[\overline{\text{SE}}_{\text{Lin},r}] \leq \mathbb{E} \left[\log_2 \left(\frac{|\mathbf{h}_{c,K+1}^H \boldsymbol{\theta}|^2 \bar{p}}{e^{-\gamma} \sum_{k=1}^K \frac{\boldsymbol{\theta}^H \mathbf{R}_{c,k} \boldsymbol{\theta}}{\text{tr}(\mathbf{R}_{d,k})}} \right) \right], \quad (30)$$

where γ is the Euler-Mascheroni constant, $\mathbf{R}_{d,k}$ are the covariance matrices of the direct channels, and

$$\mathbf{R}_{c,k} = \mathbb{E}[\mathbf{h}_{c,k} \mathbf{h}_{c,k}^H] = \text{diag}(\mathbf{a}^*) \mathbf{R}_{r,k} \text{diag}(\mathbf{a}) L_G N_B \quad (31)$$

are the covariance matrices of the cascaded channels.

Proof. See Appendix D. \square

It is important to note that the channel distribution of the direct channels $\mathbf{h}_{d,k}$, $\forall k = 1, \dots, K$ as well as the channel distribution of the weak user $\mathbf{h}_{r,K+1}$ are arbitrary and Theorem 2 holds for all distributions. Especially, the user $K+1$ which is served by the RIS can certainly have a LOS component and, hence, it is important that the bound also holds when $\mathbf{h}_{r,K+1}$ is, e.g., Rician distributed.

In the following, we analyze Theorem 2 under the assumption that all channels follow i.i.d. Rayleigh fading, i.e., $\mathbf{h}_{d/r,k} \sim \mathcal{N}_{\mathbb{C}}(\mathbf{0}, L_{d/r,k} \mathbf{I})$ $\forall k = 1, \dots, K+1$ where $L_{d/r,k}$ is the pathloss of user k .

Corollary 1. For random/statistical phase shifts when assuming i.i.d. Rayleigh fading for the channels $\mathbf{h}_{d/r,k} \sim \mathcal{N}_{\mathbb{C}}(\mathbf{0}, L_{d/r,k} \mathbf{I})$ $\forall k = 1, \dots, K+1$, the SE of linear precoding is upper bounded by

$$\mathbb{E}[\overline{\text{SE}}_{\text{Lin},r}] \leq \log_2 \left(N_B \frac{L_{r,K+1} \bar{p}}{\sum_{k=1}^K \frac{L_{r,k}}{L_{d,k}}} \right) \quad (32)$$

which is independent of N_R . For DPC, on the other hand, the SE increases monotonically with N_R according to

$$\mathbb{E}[\overline{\text{SE}}_{\text{DPC},r}] = \log_2 \left(e^{-\gamma} L_G L_{r,K+1} N_B N_R \bar{p} \right). \quad (33)$$

Proof. See Appendix E. \square

It is important to note that both, random and statistical phase shifts, lead to the same expression for the upper bound in the case of i.i.d. Rayleigh fading. Hence, both random and statistical phase shifts have a clear limitation in the sense that the SE is bounded by a term which does not depend on the number of reflecting elements N_R . Therefore, the mitigation of the users $k \leq K$ on the user $K+1$ can be so large that there is no improvement anymore when increasing the number of reflecting elements N_R . This is clearly different from DPC for which $\overline{\text{SE}}_{\text{DPC},r}$ scales linearly inside the logarithm w.r.t. N_R for random/statistical phase shifts.

Additionally, when solely maximizing the channel gain of the weak user $K + 1$ we obtain the following result.

Corollary 2. *When solely optimizing the channel gain of the weak user $K + 1$, i.e., choosing $\theta = \exp(j \arg(\mathbf{h}_{c,K+1}))$, then, under the assumption of i.i.d. Rayleigh fading for the channels $\mathbf{h}_{d/r,k} \sim \mathcal{N}_{\mathbb{C}}(\mathbf{0}, L_{d/r,k} \mathbf{I}) \forall k = 1, \dots, K + 1$, the SE of linear precoding is upper bounded by*

$$\mathbb{E}[\overline{SE}_{Lin,r}] \leq \log_2 \left(\frac{\pi e^\gamma}{4} N_R N_B \frac{L_{r,K+1} \bar{p}}{\sum_{k=1}^K \frac{L_{r,k}}{L_{d,k}}} \right) \quad (34)$$

whereas for DPC the SE is lower bounded according to

$$\mathbb{E}[\overline{SE}_{DPC,r}] \geq \log_2 (e^{-\gamma} L_G L_{r,K+1} N_B N_R^2 \bar{p}). \quad (35)$$

Proof. See Appendix F and Appendix G. \square

We see again a clear limitation for linear precoding in the sense that solely optimizing the weak user's channel gain is upper bounded by a rate expression which scales only linearly with N_R inside the logarithm. For DPC, this is the optimal solution and the SE scales quadratically within the logarithm.

In summary, it is important to suppress the mitigation term, which is possible in case of instantaneous CSI for $N_R > K$. Under statistical CSI, suppressing the mitigation is only possible if the sum of the covariance matrices $\mathbf{R}_{c,k}$ of the strong users do not span the whole space $\mathbb{C}^{N_R \times N_R}$ which can only happen for correlated Rayleigh fading. This analysis, however, will be subject to future work. In this article, only i.i.d. Rayleigh fading is considered in which linear precoding has a major disadvantage when statistical or random phase shifts are considered.

V. EQUIVALENCE OF DPC AND LINEAR PRECODING

Taking into account all the results of the last section, under the assumption of orthogonal strong direct users' channels \mathbf{H}_d^s , an orthogonal BS-RIS channel ($\mathbf{b} \in \text{null}(\mathbf{H}_d^s)$), and that the strong users are considerable far away from the RIS such that the reflections can be neglected, DPC and linear precoding perform equally w.r.t. the sum-SE. This can also be seen by rewriting the composite channel matrix as [cf. (6)]

$$\mathbf{H} = \mathbf{H}_d + \mathbf{H}_c \theta \mathbf{b}^H = \begin{bmatrix} \Sigma_s & \mathbf{H}_c^s \theta \\ \mathbf{0} & \mathbf{h}_{c,K+1}^H \theta \end{bmatrix} \begin{bmatrix} \mathbf{V}_s^H \\ \mathbf{b}^H \end{bmatrix} \quad (36)$$

where $\mathbf{U}_s = \mathbf{I}$ of the SVD of $\mathbf{H}_d^s = \mathbf{U}_s \Sigma_s \mathbf{V}_s^H$ as the direct channel users are orthogonal. Because $\mathbf{H}_c^s \theta$ is negligible by assumption and $\mathbf{b} \perp \mathbf{V}_s^s$, the channel matrix is orthogonal. These are a lot of assumptions (which are more likely to be fulfilled for large N_B), and in general, DPC will lead to superior performance.

VI. RESULTS

For the simulations we consider, similar to [38], one BS at (0, 0, 10) m with N_B antennas together with an RIS at (100, 0, 10) m which has N_R reflecting elements. We assume $K + 1 = 4$ single-antenna users on a height of 1.5 m which are uniformly distributed in a circle with radius 5 m centered at (95, 10, 1.5) m. We use the logarithmic pathloss model

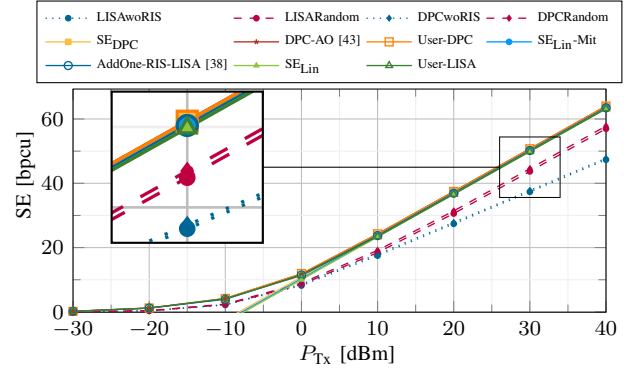


Figure 2. SE evaluation with $N_B = 12$ and $N_R = 64$.

$L_{dB} = \alpha + \beta 10 \log_{10}(\frac{d}{m})$ for all channels where d is the distance in meter. The values for α and β are chosen as in [40] which are according to the 3GPP model. For the pathloss, we choose $L_{dB,weak} = 35.1 + 36.7 \log_{10}(d/m)$ for the direct channel. For the channel between the RIS and the users we assume a stronger channel and use $L_{dB,strong} = 37.51 + 22 \log_{10}(d/m)$. The weak user which should be served via the RIS has a significantly degraded direct channel (additional pathloss of 60 dB). For the direct and the RIS-user channels, we assume i.i.d. Rayleigh fading whereas for the BS-RIS channel, we assume a LOS channel corresponding to the outer product of two half-wavelength uniform linear array (ULA) vectors where the angle of arrival (AoA) and the angle of departure (AoD) are both given by $\frac{\pi}{2}$. The pathloss for the LOS BS-RIS channel is given by $L_{dB,LOS} = 30 + 22 \log_{10}(d/m)$. In all simulations, a noise power of $\sigma^2 = -110$ dBm is used.

We evaluate the asymptotic sum-SE expressions (18) and (19) derived in this article where the optimal solution of (19) w.r.t. θ is given in closed-form by $\exp(j \angle(\mathbf{h}_{c,K+1}))$, referred to as \mathbf{SE}_{DPC} . For (18), we choose $\exp(j \angle(\mathbf{h}_{c,K+1}))$ as an initialization to the element-wise algorithm of [41], [42] that takes the mitigation term into account, referred to as $\mathbf{SE}_{Lin-Mit}$. We compare this with simply taking the initial solution and neglecting the mitigation, referred to as \mathbf{SE}_{Lin} . As a comparison, we use the **DPC-AO** of [43] with 10 random initial phase shifts of which the best solution is taken. For linear precoding, we choose the **AddOne-RIS-LISA** algorithm of [38], which converges to zero-forcing if $N_B \geq K + 1$ and $P_{Tx} \rightarrow \infty$. Additionally, we evaluate two user-based methods in which the phases of the RIS are aligned such that the channel gain of a particular user k is maximized. This is done for all users and conventional DPC as well as conventional linear precoding (with linear successive allocation (LISA)) is used for all the $k = 1, 2, \dots, K + 1$ phase shifts. Afterward, the best sum-SE is taken and we obtain **User-DPC** and **User-LISA**, respectively. For linear precoding, we use LISA [44], which converges to zero-forcing for $N_B \geq K + 1$ and $P_{Tx} \rightarrow \infty$. Additionally, we compare all the methods with random phase shifts as well as the situation where no RIS is present. Both are evaluated for DPC as well as LISA and we obtain **LISAwORIS**, **DPCwORIS**, **LISARandom**, and **DPCRandom**.

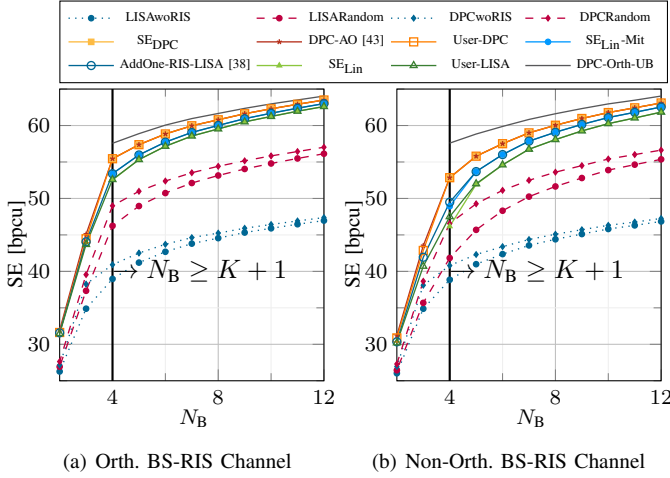


Figure 3. SE evaluation with $N_R = 64$ and $P_{Tx} = 40$ dBm.

In Fig. 2, we can see that all algorithms match the high-SNR expressions after around 10 dBm. Additionally, we can observe that the slope of the curves, when including the RIS, are higher since, additionally, the weak user is allocated. Furthermore, all optimized algorithms show similar performance as we already have $N_B = 12$ BS antennas.

In Fig. 3 we further analyze the impact of the number of BS antennas. Here, we additionally included **DPC-Orth-UB** which is SE_{DPC} for an orthogonal BS-RIS channel as well as orthogonal direct user channels and, hence, serves as an upper bound. In Fig 3(a), we artificially set the vector \mathbf{b} to be orthogonal to the strong users' direct channels whereas in Fig. 3(b), we don't have this artificial scenario and, therefore, the BS-RIS channel is not orthogonal to the direct channel. While for $N_B \rightarrow \infty$ the algorithms converge to the same values in both plots, we can see that an orthogonal BS-RIS channel is clearly beneficial for the performance (especially for lower N_B values), which is particularly pronounced for linear precoding.

In Fig. 4, we further analyze the orthogonality of the BS-RIS channel for $N_B = K + 1 = 4$. We express the orthogonality by constructing $\mathbf{b}' = \frac{\mathbf{V}_s^H \mathbf{1}}{\|\mathbf{V}_s^H \mathbf{1}\|_2} + \xi \frac{\mathbf{v}^\perp}{\|\mathbf{v}^\perp\|_2}$ where \mathbf{v}^\perp is orthogonal to $\text{range}(\mathbf{V}_s)$. Afterwards \mathbf{b} is obtained by

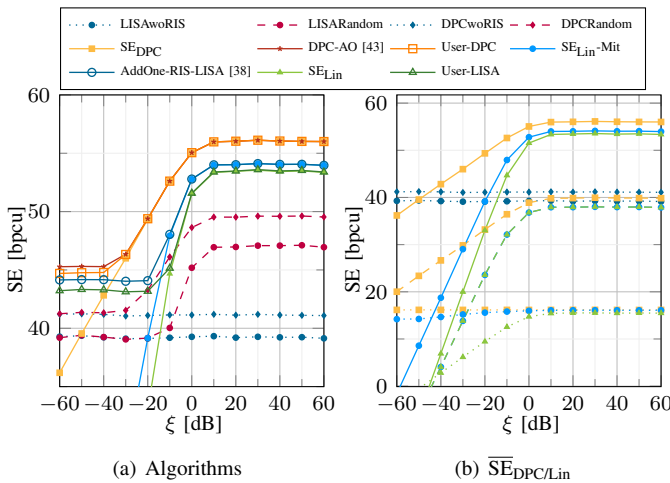


Figure 4. SE evaluation with $P_{Tx} = 40$ dBm, $N_R = 64$, and $N_B = 4$.

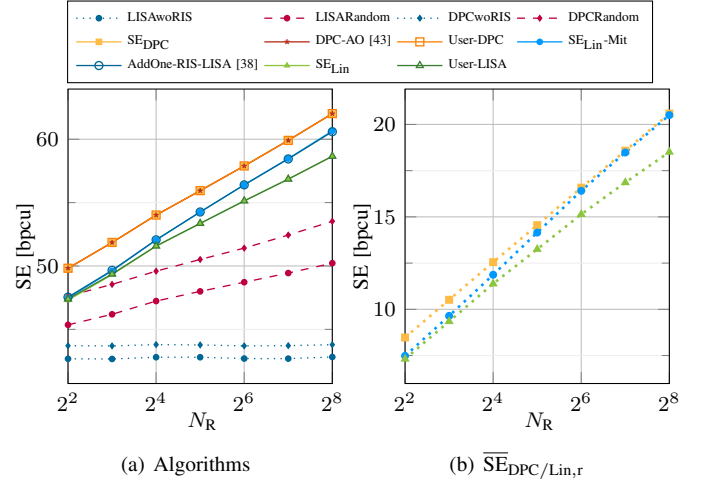


Figure 5. SE evaluation with $P_{Tx} = 40$ dBm and $N_B = 6$.

normalizing \mathbf{b}' , i.e., $\mathbf{b} = \frac{\mathbf{b}'}{\|\mathbf{b}'\|_2}$. We can see in 4(a) that an orthogonal BS-RIS channel is clearly beneficial for all methods. The linear precoding methods are especially sensitive for this orthogonality in comparison to the DPC based schemes which are more robust in this regard.

We further analyze this behavior in Fig. 4(b) by splitting $\overline{SE}_{DPC/Lin}(-Mit)$ (**solid**) into $\overline{SE}_{DPC/Lin,d}(-Mit)$ (**dashed**) and $\overline{SE}_{DPC/Lin,r}(-Mit)$ (**dotted**), see (18) and (19). It is apparent that $\overline{SE}_{DPC/Lin,d}$ clearly depends on the orthogonality, especially for the linear precoding methods. For high values of ξ , the orthogonal projector of $\mathbf{C}_s = \mathbf{H}_d^s \mathbf{P}_b^\perp \mathbf{H}_d^{s,H}$ vanishes and we have the same expression as in case of only the direct channels. The offset of $\overline{SE}_{DPC/Lin,d}$ to the direct channel for large values of ξ is only due to the fact that the power is divided over $K + 1 = 4$ users instead of $K = 3$ users and, hence, we obtain the offset $K \log_2(\frac{K+1}{K}) = 1.2451$ bpcu. On the other hand, when considering the terms $\overline{SE}_{Lin/DPC,r}$, only the linear methods depend on \mathbf{b} . When taking the mitigation into account, this dependence is very small, as in this scenario the RIS has enough impact on the strong users to cancel this dependence. However, the interference has to be taken actively into account as can be seen when only maximizing the weak user's channel gain. Here, $\overline{SE}_{Lin,r}$ significantly depends on the orthogonality as the direction $\mathbf{H}_d^s \mathbf{b}$ is not compensated when maximizing only the weak user's channel gain. This results in a clear degradation when the BS-RIS channel is not orthogonal.

In Fig. 5, we further investigate the ability to compensate for the channel part $\mathbf{H}_d^s \mathbf{b}$ depending on the number of reflecting elements N_R . At first, we focus on Fig. 5(a) where we can see that there is a clear gap between DPC and linear precoding. For random phase shifts as well as when neglecting the mitigation term, this gap is significantly larger as in case of having solely the direct channels. This is different for $\overline{SE}_{Lin-Mit}$ which for a low number of reflecting elements performs equal to \overline{SE}_{Lin} , whereas for a high number of elements, the gap to DPC is significantly reduced.

We analyze this behavior in 5(b) where we only plot $\overline{SE}_{DPC/Lin,r}$. Note that $\overline{SE}_{DPC/Lin,d}$ does not depend on the

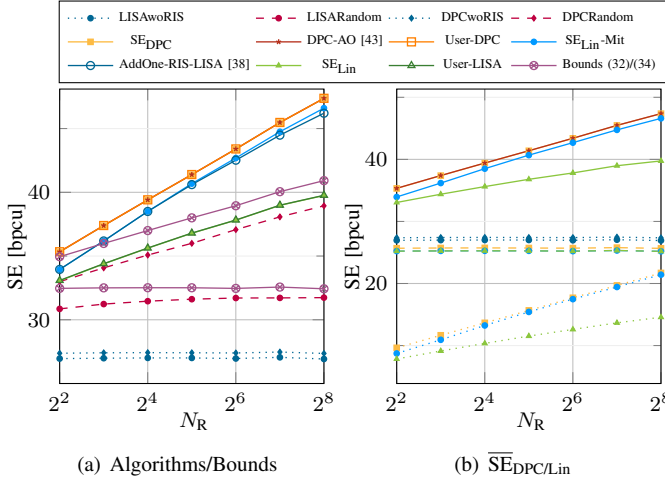


Figure 6. SE evaluation with $P_{Tx} = 40$ dBm and $N_B = 12$. Additional 20 dB pathloss for the direct channels.

reflecting elements and, hence, is constant over N_R . We can see that if the impact of the reflecting channel is low, we have $1 + \bar{\theta}^H D_s^H C_s^{-1} D_s \bar{\theta} = 1/b^H P_{H_s}^\perp b$ according to eq. (27) and maximizing the weak user's channel gain is optimal. Hence, $\overline{SE}_{Lin,r}$ and $\overline{SE}_{Lin,r}$ -Mit are overlapping and a clear gap to DPC exists. For a higher number of reflecting elements the reflecting channel has more impact and actually helps to compensate for $H_d^s b$. Therefore, $\overline{SE}_{Lin,r}$ -Mit gains a lot of performance over N_R and is very close to $\overline{SE}_{DPC,r}$. On the other hand, the increasing impact of the reflecting channel becomes problematic when the mitigation is neglected and we can already see a saturation effect of $\overline{SE}_{Lin,r}$ for a higher number of reflecting elements.

In Fig. 6, this saturation effect is investigated. To clearly see the problem of the mitigation term, we assume the direct channels to have an additional pathloss of 20 dB. In Fig 6(a) we can see that the mitigation term plays a fundamental role for the system performance. For random and statistical phase shifts, the SE stays constant whereas solely maximizing the weak user's channel gain scales only linearly w.r.t. N_R inside the logarithm. This is further illustrated by plotting the bounds in (32) and (34) which explain these effects. In Fig. 6(b) this is further supported by recognizing that $\overline{SE}_{Lin,r}$ is clearly limited when the mitigation is not taken into account. On the other hand, when the mitigation is taken into account, we can expect the same scaling behavior as DPC.

VII. CONCLUSION

We have analyzed a scenario in which a group of strong users and a group of weak users are supported by a RIS with a LOS dominated BS-RIS channel. Interestingly, linear precoding differs significantly from DPC, i.e., that it suffers from an mitigation term which completely vanishes in case of DPC. This is especially pronounced when considering random/statistical phase shifts under i.i.d. Rayleigh fading. A number of assumptions have to be fulfilled for DPC and linear precoding to perform equally, e.g., the BS-RIS channel has to be orthogonal to the users with non-negligible direct channels which is generally important for the performance. In future

works, it is analyzed how these results can be extended to a scenario with an increased rank of the BS-RIS channel.

APPENDIX

A. Effective Channel Gains of ZF

We start by rewriting the Gram channel matrix

$$HH^H = \begin{bmatrix} C_s & \mathbf{0} \\ \mathbf{0}^T & 0 \end{bmatrix} + D\bar{\theta}\bar{\theta}^H D^H. \quad (37)$$

From the definitions (11) and (13) it follows that

$$D\bar{\theta} = \begin{bmatrix} D_s \bar{\theta} \\ h_{c,K+1}^H \theta \end{bmatrix} \quad (38)$$

and we can express the Gram channel matrix as

$$HH^H = \begin{bmatrix} C_s + D_s \bar{\theta}\bar{\theta}^H D_s^H & D_s \bar{\theta}\bar{\theta}^H h_{c,K+1} \\ h_{c,K+1}^H \theta \bar{\theta}^H D_s^H & |h_{c,K+1}^H \theta|^2 \end{bmatrix}. \quad (39)$$

Applying the block matrix inversion, we have

$$\begin{aligned} (HH^H)^{-1} &= \begin{bmatrix} C_s + D_s \bar{\theta}\bar{\theta}^H D_s^H & D_s \bar{\theta}\bar{\theta}^H h_{c,K+1} \\ h_{c,K+1}^H \theta \bar{\theta}^H D_s^H & |h_{c,K+1}^H \theta|^2 \end{bmatrix}^{-1} \\ &= \begin{bmatrix} C_s^{-1} & -C_s^{-1} D_s \bar{\theta} \frac{\theta^H h_{c,K+1}}{|h_{c,K+1}^H \theta|^2} \\ -\frac{h_{c,K+1}^H \theta}{|h_{c,K+1}^H \theta|^2} \bar{\theta}^H D_s^H C_s^{-1} & \frac{1 + \bar{\theta}^H D_s^H C_s^{-1} D_s \bar{\theta}}{|h_{c,K+1}^H \theta|^2} \end{bmatrix} \end{aligned} \quad (40)$$

and, hence, we can give the inverted channel gains for zero forcing $e_k^T (HH^H)^{-1} e_k$ according to (14).

B. Asymptotic SE of DPC

Using (9) and defining

$$C = \begin{bmatrix} C_s & \mathbf{0} \\ \mathbf{0}^T & 0 \end{bmatrix}, \quad (41)$$

we can write the SE in case of DPC as

$$\begin{aligned} SE_{DPC} &= \log_2 \det(\mathbf{I} + H^H Q H) \\ &= \log_2 \det(\mathbf{I} + H H^H \bar{p}) \\ &= \log_2 \det(\mathbf{I} + C \bar{p} + D \bar{\theta} \bar{\theta}^H D^H \bar{p}) \\ &= \log_2 \det(\mathbf{I} + C \bar{p}) \\ &\quad + \log_2 \det\left(\mathbf{I} + (\mathbf{I} + C \bar{p})^{-1} D \bar{\theta} \bar{\theta}^H D^H \bar{p}\right) \\ &= \log_2 \det(\mathbf{I} + C_s \bar{p}) \\ &\quad + \log_2 \left(1 + \bar{\theta}^H D^H (\mathbf{I} + C \bar{p})^{-1} D \bar{\theta} \bar{p}\right) \\ &= \sum_{k=1}^K \log_2(1 + \lambda_k \bar{p}) \\ &\quad + \log_2 \left(1 + \sum_{k=1}^{K+1} |\bar{\theta}^H D^H u_k|^2 \frac{\bar{p}}{1 + \lambda_k \bar{p}}\right) \\ &= \sum_{k=1}^K \log_2(1 + \lambda_k \bar{p}) \\ &\quad + \log_2 \left(1 + |h_{c,K+1}^H \theta|^2 \bar{p} + \sum_{k=1}^K |\bar{\theta}^H D^H u_k|^2 \frac{\bar{p}}{1 + \lambda_k \bar{p}}\right) \end{aligned} \quad (42)$$

where λ_k denotes the k -th eigenvalue of C and $|h_{c,K+1}^H \theta|^2 \neq 0$.

C. A Lower Bound for the Exponential Integral

There are popular bounds for the exponential integral (see [45, p. 229, eq. (5.1.19) and (5.1.20)] and [46], [47]), however, all of them are not suited for our purposes in this article. Specifically, the problem with the bound of [46]

$$E_1(x)e^x > \frac{1}{2} \ln \left(1 + \frac{2}{x} \right), \quad \forall x > 0 \quad (43)$$

is the prefactor of 0.5 outside the logarithm. In [48, eq. (12)] there has been given a bound without this factor

$$E_1(x)e^x > -\gamma + \ln \left(1 + \frac{1}{x} \right), \quad \forall x > 0. \quad (44)$$

where γ is the Euler-Mascheroni constant. However, also this bound is not applicable for our problem because of the constant term $-\gamma$. Hence, we introduce a new lower bound for the exponential integral which is tighter than the one in (44) for all $x > 0$. In particular, we prove the relationship

$$E_1(x)e^x > \ln \left(1 + \frac{e^{-\gamma}}{x} \right), \quad \forall x > 0 \quad (45)$$

and we have

$$\ln \left(e^{-\gamma} + \frac{e^{-\gamma}}{x} \right) < \ln \left(1 + \frac{e^{-\gamma}}{x} \right), \quad \forall x > 0 \quad (46)$$

when comparing the bound with (44).

To show (45), we introduce the difference

$$g(x) = E_1(x) - e^{-x} \ln \left(1 + \frac{e^{-\gamma}}{x} \right) \quad (47)$$

which we show to be positive for all positive x . By exploiting the property $E_1'(x) = -E_0'(x) = -\frac{e^{-x}}{x}$ (see [45, p. 230, eq. (5.1.26) and p. 229 eq. (5.1.24)]), the first-order derivative $g'(x)$ of $g(x)$ is given by

$$g'(x) = e^{-x} \underbrace{\left(\ln \left(1 + \frac{e^{-\gamma}}{x} \right) - \frac{1}{e^{-\gamma} + x} \right)}_{\tilde{g}'(x)}.$$

Taking the derivative of $\tilde{g}'(x)$, we obtain

$$\frac{d}{dx} \tilde{g}'(x) = \frac{-e^{-2\gamma} + x(1 - e^{-\gamma})}{x(x + e^{-\gamma})^2}. \quad (48)$$

This expression is equal to zero for $x = \frac{e^{-2\gamma}}{1 - e^{-\gamma}} \approx 0.719$, negative for $x < \frac{e^{-2\gamma}}{1 - e^{-\gamma}}$ and positive for $x > \frac{e^{-2\gamma}}{1 - e^{-\gamma}}$. It follows, that $\tilde{g}'(x)$ is monotonically decreasing for $x < \frac{e^{-2\gamma}}{1 - e^{-\gamma}}$, having a minimum at $x = \frac{e^{-2\gamma}}{1 - e^{-\gamma}}$ and then monotonically increasing for $x > \frac{e^{-2\gamma}}{1 - e^{-\gamma}}$. Additionally, we have

$$\lim_{x \rightarrow 0^+} \tilde{g}'(x) = \infty, \quad \lim_{x \rightarrow \infty} \tilde{g}'(x) = 0.$$

Summarizing the information about $\tilde{g}'(x)$, we can infer that $\tilde{g}'(x)$ has exactly one zero in the interval $x_0 \in \left(0, \frac{e^{-2\gamma}}{1 - e^{-\gamma}} \right)$. For $x < x_0$, $\tilde{g}'(x)$ is positive, whereas for $x > x_0$, $\tilde{g}'(x)$ is negative. Because $g'(x) = e^{-x} \tilde{g}'(x)$, $g'(x)$ also has exactly one zero in the interval $x_0 \in \left(0, \frac{e^{-2\gamma}}{1 - e^{-\gamma}} \right)$, is positive for $x < x_0$, and negative for $x > x_0$. Hence, the difference $g(x)$ has exactly one maximum at $x_0 \in \left(0, \frac{e^{-2\gamma}}{1 - e^{-\gamma}} \right)$, is strictly

increasing for $x < x_0$, and strictly decreasing for $x > x_0$. It follows that we only have to show that $\lim_{x \rightarrow 0^+} g(x) \geq 0$ and $\lim_{x \rightarrow \infty} g(x) \geq 0$. For $x \rightarrow \infty$, one can directly see from (47) that

$$\lim_{x \rightarrow \infty} g(x) = 0.$$

For $x \rightarrow 0^+$ the situation is less clear. We use the series representation of $E_1(x)$ from [45, p.229, eq. (5.1.11)] and write $g(x)$ as

$$g(x) = -\gamma - \ln(x) - \sum_{k=1}^{\infty} \frac{(-x)^k}{kk!} - e^{-x} \ln \left(1 + \frac{e^{-\gamma}}{x} \right).$$

Because

$$\lim_{x \rightarrow 0^+} \left[-\ln(x) - e^{-x} \ln \left(1 + \frac{e^{-\gamma}}{x} \right) \right] = \gamma \quad (49)$$

and furthermore, with the geometric series, we have

$$\begin{aligned} \lim_{x \rightarrow 0^+} \sum_{k=1}^{\infty} \frac{(-x)^k}{kk!} &\leq \lim_{x \rightarrow 0^+} \left[-1 + \sum_{k=0}^{\infty} x^k \right] \\ &= \lim_{x \rightarrow 0^+} \left[\frac{1}{1-x} - 1 \right] = 0, \end{aligned} \quad (50)$$

as well as

$$\begin{aligned} \lim_{x \rightarrow 0^+} \sum_{k=1}^{\infty} \frac{(-x)^k}{kk!} &\geq \lim_{x \rightarrow 0^+} \left[1 - \sum_{k=0}^{\infty} x^k \right] \\ &= \lim_{x \rightarrow 0^+} \left[1 - \frac{1}{1-x} \right] = 0. \end{aligned} \quad (51)$$

It follows that

$$\lim_{x \rightarrow 0^+} g(x) = 0.$$

Hence, we have

$$g(x) > 0, \quad \forall x > 0 \quad (52)$$

and the upper bound in (45) holds.

D. Ergodic Upper Bound for Linear Precoding

In this section, we derive an upper bound for $\mathbb{E}[\overline{\text{SE}}_{\text{Lin},r}]$ defined in (18). This upper bound holds for random phase shifts, statistical phase shifts as well as for phase shifts which are only based on optimizing the numerator $|\mathbf{h}_{c,K+1}^H \boldsymbol{\theta}|^2$. All these choices have in common that they are independent of the channels of user $k = 1, \dots, K$. Firstly, we derive a lower bound for $\bar{\boldsymbol{\theta}}^H \mathbf{D}_s^H \mathbf{C}_s^{-1} \mathbf{D}_s \bar{\boldsymbol{\theta}}$ with the matrix inversion lemma by

$$\begin{aligned} &\bar{\boldsymbol{\theta}}^H \mathbf{D}_s^H \mathbf{C}_s^{-1} \mathbf{D}_s \bar{\boldsymbol{\theta}} = \\ &= \bar{\boldsymbol{\theta}}^H \mathbf{D}_s^H \left((\mathbf{H}_d^s \mathbf{H}_d^{s,H}) - \mathbf{H}_d^s \mathbf{b} \mathbf{b}^H \mathbf{H}_d^{s,H} \right)^{-1} \mathbf{D}_s \bar{\boldsymbol{\theta}} \\ &= \bar{\boldsymbol{\theta}}^H \mathbf{D}_s^H (\mathbf{H}_d^s \mathbf{H}_d^{s,H})^{-1} \mathbf{D}_s \bar{\boldsymbol{\theta}} + \frac{|\mathbf{b}^H \mathbf{H}_d^s (\mathbf{H}_d^s \mathbf{H}_d^{s,H})^{-1} \mathbf{D}_s \bar{\boldsymbol{\theta}}|^2}{1 - \mathbf{b}^H \mathbf{H}_d^s (\mathbf{H}_d^s \mathbf{H}_d^{s,H})^{-1} \mathbf{H}_d^s \mathbf{b}} \\ &= \bar{\boldsymbol{\theta}}^H \mathbf{D}_s^H (\mathbf{H}_d^s \mathbf{H}_d^{s,H})^{-1} \mathbf{D}_s \bar{\boldsymbol{\theta}} + \frac{|\mathbf{b}^H \mathbf{H}_d^s + \mathbf{D}_s \bar{\boldsymbol{\theta}}|^2}{1 - \mathbf{b}^H \mathbf{P}_{\mathbf{H}_d^s} \mathbf{b}} \end{aligned} \quad (53)$$

where we used the definition of the matrix $\mathbf{C}_s = \mathbf{H}_d^s \mathbf{P}_b^\perp \mathbf{H}_d^{s,H}$, the pseudoinverse $\mathbf{H}_d^{s,+} = \mathbf{H}_d^{s,H} (\mathbf{H}_d^s \mathbf{H}_d^{s,H})^{-1}$, and the projector $\mathbf{P}_{\mathbf{H}_d^{s,H}} = \mathbf{H}_d^{s,H} (\mathbf{H}_d^s \mathbf{H}_d^{s,H})^{-1} \mathbf{H}_d^s = \mathbf{H}_d^{s,+} \mathbf{H}_d^s$. With the definition of the matrix $\mathbf{D}_s = [\mathbf{H}_c^s, \mathbf{H}_d^s \mathbf{b}]$ we can express the first term of (53) as

$$\begin{aligned} \bar{\boldsymbol{\theta}}^H \mathbf{D}_s^H (\mathbf{H}_d^s \mathbf{H}_d^{s,H})^{-1} \mathbf{D}_s \bar{\boldsymbol{\theta}} &= \boldsymbol{\theta}^H \mathbf{H}_c^s \mathbf{H}_c^s (\mathbf{H}_d^s \mathbf{H}_d^{s,H})^{-1} \mathbf{H}_c^s \boldsymbol{\theta} \\ &+ 2\text{Re}(\mathbf{b}^H \mathbf{H}_d^{s,+} \mathbf{H}_c^s \boldsymbol{\theta}) + \mathbf{b}^H \mathbf{P}_{\mathbf{H}_d^{s,H}} \mathbf{b} \end{aligned} \quad (54)$$

and the second term of (53) as

$$\begin{aligned} \frac{|\mathbf{b}^H \mathbf{H}_d^{s,+} \mathbf{D}_s \bar{\boldsymbol{\theta}}|^2}{1 - \mathbf{b}^H \mathbf{P}_{\mathbf{H}_d^{s,H}} \mathbf{b}} &= \frac{|\mathbf{b}^H \mathbf{H}_d^{s,+} \mathbf{H}_c^s \boldsymbol{\theta}|^2}{1 - \mathbf{b}^H \mathbf{P}_{\mathbf{H}_d^{s,H}} \mathbf{b}} \\ &+ \frac{2\text{Re}(\mathbf{b}^H \mathbf{H}_d^{s,+} \mathbf{H}_c^s \boldsymbol{\theta}) \mathbf{b}^H \mathbf{P}_{\mathbf{H}_d^{s,H}} \mathbf{b}}{1 - \mathbf{b}^H \mathbf{P}_{\mathbf{H}_d^{s,H}} \mathbf{b}} + \frac{(\mathbf{b}^H \mathbf{P}_{\mathbf{H}_d^{s,H}} \mathbf{b})^2}{1 - \mathbf{b}^H \mathbf{P}_{\mathbf{H}_d^{s,H}} \mathbf{b}}. \end{aligned} \quad (55)$$

Finding a common denominator for the terms (54) and (55) and plugging them into (53) results in

$$\begin{aligned} \bar{\boldsymbol{\theta}}^H \mathbf{D}_s^H \mathbf{C}_s^{-1} \mathbf{D}_s \bar{\boldsymbol{\theta}} &= \\ &= \boldsymbol{\theta}^H \mathbf{H}_c^s \mathbf{H}_c^s (\mathbf{H}_d^s \mathbf{H}_d^{s,H})^{-1} \mathbf{H}_c^s \boldsymbol{\theta} \\ &+ \frac{2\text{Re}(\mathbf{b}^H \mathbf{H}_d^{s,+} \mathbf{H}_c^s \boldsymbol{\theta}) + \mathbf{b}^H \mathbf{P}_{\mathbf{H}_d^{s,H}} \mathbf{b} + |\mathbf{b}^H \mathbf{H}_d^{s,+} \mathbf{H}_c^s \boldsymbol{\theta}|^2}{1 - \mathbf{b}^H \mathbf{P}_{\mathbf{H}_d^{s,H}} \mathbf{b}} \\ &= \boldsymbol{\theta}^H \mathbf{H}_c^s \mathbf{H}_c^s (\mathbf{H}_d^s \mathbf{H}_d^{s,H})^{-1} \mathbf{H}_c^s \boldsymbol{\theta} \\ &+ \frac{|\mathbf{b}^H \mathbf{H}_d^{s,+} \mathbf{H}_c^s \boldsymbol{\theta} + 1|^2 - 1 + \mathbf{b}^H \mathbf{P}_{\mathbf{H}_d^{s,H}} \mathbf{b}}{1 - \mathbf{b}^H \mathbf{P}_{\mathbf{H}_d^{s,H}} \mathbf{b}} \\ &\geq \boldsymbol{\theta}^H \mathbf{H}_c^s \mathbf{H}_c^s (\mathbf{H}_d^s \mathbf{H}_d^{s,H})^{-1} \mathbf{H}_c^s \boldsymbol{\theta} - 1 \end{aligned} \quad (56)$$

where we used that $1 - \mathbf{b}^H \mathbf{P}_{\mathbf{H}_d^{s,H}} \mathbf{b} > 0$. With (56), we can upper bound the ergodic rate as

$$\begin{aligned} \mathbb{E}[\overline{\text{SE}}_{\text{Lin},r}] &= \mathbb{E} \left[\log_2 \left(\frac{|\mathbf{h}_{c,K+1}^H \boldsymbol{\theta}|^2 \bar{p}}{1 + \bar{\boldsymbol{\theta}}^H \mathbf{D}_s^H \mathbf{C}_s^{-1} \mathbf{D}_s \bar{\boldsymbol{\theta}}} \right) \right] \\ &\leq \mathbb{E} \left[\log_2 \left(\frac{|\mathbf{h}_{c,K+1}^H \boldsymbol{\theta}|^2 \bar{p}}{\boldsymbol{\theta}^H \mathbf{H}_c^s \mathbf{H}_c^s (\mathbf{H}_d^s \mathbf{H}_d^{s,H})^{-1} \mathbf{H}_c^s \boldsymbol{\theta}} \right) \right] \\ &= \mathbb{E} \left[\log_2 \left(|\mathbf{h}_{c,K+1}^H \boldsymbol{\theta}|^2 \bar{p} \right) - \log_2 \left(\mathbf{h}^H (\mathbf{H}_d^s \mathbf{H}_d^{s,H})^{-1} \mathbf{h} \right) \right] \end{aligned} \quad (57)$$

where we introduced the definition

$$\mathbf{h} = \mathbf{H}_c^s \boldsymbol{\theta}. \quad (58)$$

The mitigation term

$$\mathbb{E}[\text{Mit}] = \mathbb{E}_{\mathbf{H}_r, \boldsymbol{\theta}} \left[\mathbb{E}_{\mathbf{H}_d^s | \mathbf{H}_r, \boldsymbol{\theta}} \left[\log_2 \left(\mathbf{h}^H (\mathbf{H}_d^s \mathbf{H}_d^{s,H})^{-1} \mathbf{h} \right) \right] \right] \quad (59)$$

is analyzed in the following. For this, we define the matrix

$$\mathbf{H}_d^{s,H} = [\mathbf{h}_{d,1}, \dots, \mathbf{h}_{d,K}] = [\tilde{\mathbf{h}}_{d,1}, \dots, \tilde{\mathbf{h}}_{d,K}] \boldsymbol{\Sigma}_d = \tilde{\mathbf{H}}_d^{s,H} \boldsymbol{\Sigma}_d \quad (60)$$

where $\boldsymbol{\Sigma}_d$ is a diagonal matrix with $[\boldsymbol{\Sigma}_d]_{k,k} = \sqrt{\text{tr}(\mathbf{R}_{d,k})}$ and $\tilde{\mathbf{H}}_d^{s,H} = [\tilde{\mathbf{h}}_{d,1}, \dots, \tilde{\mathbf{h}}_{d,K}]$ are the normalized direct channels with unit-variance. Further defining $\tilde{\mathbf{h}} = \boldsymbol{\Sigma}_d^{-1} \mathbf{h}$, we can express the quadratic form within the logarithm in (59) as

$$\mathbf{h}^H (\mathbf{H}_d^s \mathbf{H}_d^{s,H})^{-1} \mathbf{h} = \tilde{\mathbf{h}}^H (\tilde{\mathbf{H}}_d^s \tilde{\mathbf{H}}_d^{s,H})^{-1} \tilde{\mathbf{h}}. \quad (61)$$

Introducing the eigenvalue decomposition (EVD) of $(\tilde{\mathbf{H}}_d^s \tilde{\mathbf{H}}_d^{s,H})^{-1} = \sum_{k=1}^K \mathbf{u}_k \mathbf{u}_k^H \frac{1}{\lambda_k}$ and applying the weighted harmonic-arithmetic mean inequality, we obtain

$$\begin{aligned} \tilde{\mathbf{h}}^H (\tilde{\mathbf{H}}_d^s \tilde{\mathbf{H}}_d^{s,H})^{-1} \tilde{\mathbf{h}} &= \sum_{k=1}^K \left| \tilde{\mathbf{h}}^H \mathbf{u}_k \right|^2 \frac{1}{\lambda_k} \geq \frac{\left(\sum_{k=1}^K \left| \tilde{\mathbf{h}}^H \mathbf{u}_k \right|^2 \right)^2}{\sum_{k=1}^K \left| \tilde{\mathbf{h}}^H \mathbf{u}_k \right|^2 \lambda_k} \\ &= \frac{\|\tilde{\mathbf{h}}\|^4}{\tilde{\mathbf{h}}^H (\tilde{\mathbf{H}}_d^s \tilde{\mathbf{H}}_d^{s,H}) \tilde{\mathbf{h}}}. \end{aligned} \quad (62)$$

Using this result and recognizing that $\log_2(\frac{a}{x})$ is convex w.r.t. $x > 0$ for any positive a , we can bound the inner expectation in (59) by applying Jensen's inequality as

$$\begin{aligned} &\mathbb{E}_{\mathbf{H}_d^s | \mathbf{H}_r, \boldsymbol{\theta}} \left[\log_2 \left(\mathbf{h}^H (\mathbf{H}_d^s \mathbf{H}_d^{s,H})^{-1} \mathbf{h} \right) \right] \\ &\geq \mathbb{E}_{\mathbf{H}_d^s | \mathbf{H}_r, \boldsymbol{\theta}} \left[\log_2 \left(\frac{\|\tilde{\mathbf{h}}\|^4}{\tilde{\mathbf{h}}^H (\tilde{\mathbf{H}}_d^s \tilde{\mathbf{H}}_d^{s,H}) \tilde{\mathbf{h}}} \right) \right] \\ &\geq \log_2 \left(\frac{\|\tilde{\mathbf{h}}\|^4}{\tilde{\mathbf{h}}^H \mathbb{E}_{\mathbf{H}_d^s | \mathbf{H}_r, \boldsymbol{\theta}} \left[(\tilde{\mathbf{H}}_d^s \tilde{\mathbf{H}}_d^{s,H}) \right] \tilde{\mathbf{h}}} \right) \\ &= \log_2 \left(\frac{\|\tilde{\mathbf{h}}\|^4}{\tilde{\mathbf{h}}^H \mathbf{I} \tilde{\mathbf{h}}} \right) \\ &= \log_2 \left(\|\tilde{\mathbf{h}}\|^2 \right) \\ &= \log_2 \left(\sum_{k=1}^K \frac{|h_k|^2}{\text{tr}(\mathbf{R}_{d,k})} \right). \end{aligned} \quad (63)$$

As \mathbf{H}_r^s is assumed to be independent of \mathbf{H}_d^s and it is additionally assumed that the phases are chosen independent of \mathbf{H}_r^s (either random, based on the statistics or only dependent of $\mathbf{h}_{r,K+1}$), we have $\mathbb{E}[\mathbf{H}_d^s \mathbf{H}_d^{s,H} | \mathbf{H}_r, \boldsymbol{\theta}] = \mathbb{E}[\mathbf{H}_d^s \mathbf{H}_d^{s,H}]$. As the users are pairwise independent and the variances are normalized to unit-norm, $\mathbb{E}[\mathbf{H}_d^s \mathbf{H}_d^{s,H}] = \mathbf{I}$ holds. Analyzing (63), we observe with (58) that given $\boldsymbol{\theta}$, the variable $h_k = \mathbf{h}_{c,k}^H \boldsymbol{\theta}$ is a sum of Gaussian random variables. This holds because we have $\mathbf{h}_{r,k} \sim \mathcal{N}_{\mathbb{C}}(\mathbf{0}, \mathbf{R}_{r,k})$ and from $\mathbf{h}_{c,k}^H = \sqrt{N_B L_G} \mathbf{h}_{r,k}^H \text{diag}(\mathbf{a})$, it directly follows that also $\mathbf{h}_{c,k} \sim \mathcal{N}_{\mathbb{C}}(\mathbf{0}, \mathbf{R}_{c,k})$ with

$$\mathbf{R}_{c,k} = \mathbb{E}[\mathbf{h}_{c,k} \mathbf{h}_{c,k}^H] = \text{diag}(\mathbf{a}^*) \mathbf{R}_{r,k} \text{diag}(\mathbf{a}) L_G N_B. \quad (64)$$

Note that we assume $\boldsymbol{\theta}$ to be independent of $\mathbf{h}_{r,k}$ for $k \leq K$ and, hence, h_k is again Gaussian distributed with mean and variance

$$\mathbb{E}[h_k] = 0, \quad \text{var}[h_k] = \mathbb{E} \left[|\mathbf{h}_{c,k}^H \boldsymbol{\theta}|^2 \right] = \boldsymbol{\theta}^H \mathbf{R}_{c,k} \boldsymbol{\theta}. \quad (65)$$

Therefore, defining

$$\xi_k = \frac{2}{\boldsymbol{\theta}^H \mathbf{R}_{c,k} \boldsymbol{\theta}} |h_k|^2 \sim \chi^2(2), \quad (66)$$

ξ_k is chi-squared distributed with two degrees of freedom. Combining these observations with the lower bound in (63), we can lower bound the expression in (59) by

$$\mathbb{E}[\text{Mit}] \geq \mathbb{E}_{\boldsymbol{\theta}} \left[\mathbb{E}_{\xi_{1:K}} \left[\log_2 \left(\sum_{k=1}^K \alpha_k \xi_k \right) \right] \right] \quad (67)$$

where $\alpha_k = \boldsymbol{\theta}^H \mathbf{R}_{c,k} \boldsymbol{\theta} / (2 \operatorname{tr}(\mathbf{R}_{d,k}))$, $\xi_{1:K} = \xi_1, \xi_2, \dots, \xi_K$. The lower bound in (67) will be further bounded by successively evaluating the expression based on the chain rule of probabilities where we first assume $K \geq 2$. Starting with ξ_1 , the inner expectation in (67) can be written as

$$\begin{aligned} & \mathbb{E}_{\xi_{1:K}} \left[\log_2 \left(\sum_{k=1}^K \alpha_k \xi_k \right) \right] \\ &= \mathbb{E}_{\xi_{2:K}} \left[\mathbb{E}_{\xi_1} \left[\log_2 (b_1 + \alpha_1 \xi_1) \mid \xi_{2:K} \right] \right]. \end{aligned} \quad (68)$$

where we additionally introduced the notation

$$b_1 = \sum_{k=2}^K \alpha_k \xi_k. \quad (69)$$

Using the definition of the pdf of a chi-squared random variable with two degrees of freedom $f_{\xi_1}(\xi_1) = \frac{1}{2} e^{-\frac{\xi_1}{2}}$, the inner expectation of (68) can be expressed as

$$\begin{aligned} & \mathbb{E}_{\xi_1} \left[\log_2 (b_1 + \alpha_1 \xi_1) \mid \xi_{2:K} \right] = \\ &= \int_{-\infty}^{\infty} \log_2 (b_1 + \alpha_1 \xi_1) f_{\xi_1}(\xi_1) d\xi_1 \\ &= \frac{1}{2 \ln(2)} \int_0^{\infty} \ln(b_1 + \alpha_1 \xi_1) e^{-\frac{\xi_1}{2}} d\xi_1 \\ &\stackrel{(a)}{=} \frac{1}{2 \ln(2)} \left(\left[-2e^{-\frac{\xi_1}{2}} \ln(b_1 + \alpha_1 \xi_1) \right]_0^{\infty} \right. \\ &\quad \left. - \int_0^{\infty} \frac{-2\alpha_1 e^{-\frac{\xi_1}{2}}}{b_1 + \alpha_1 \xi_1} d\xi_1 \right) \\ &= \frac{1}{2 \ln(2)} \left(2 \ln(b_1) + \int_0^{\infty} \frac{e^{-\frac{\xi_1}{2}}}{\frac{b_1}{2\alpha_1} + \frac{\xi_1}{2}} d\xi_1 \right) \\ &\stackrel{(b)}{=} \frac{1}{2 \ln(2)} \left(2 \ln(b_1) + \int_{\frac{b_1}{2\alpha_1}}^{\infty} \frac{e^{-(u - \frac{b_1}{2\alpha_1})}}{u} 2 du \right) \\ &= \frac{1}{2 \ln(2)} \left(2 \ln(b_1) + 2e^{\frac{b_1}{2\alpha_1}} \int_{\frac{b_1}{2\alpha_1}}^{\infty} \frac{e^{-u}}{u} du \right) \\ &= \frac{1}{\ln(2)} \left(\ln(b_1) + e^{\frac{b_1}{2\alpha_1}} E_1 \left(\frac{b_1}{2\alpha_1} \right) \right) \end{aligned} \quad (70)$$

where we used integration by parts in (a) and integration by substitution in (b). In the last line, $E_1(x)$ is defined as the exponential integral. The bounds for $E_1(x)$ in [45, p. 229, eq. (5.1.20)] are not suited for our purposes and, hence, we derived a new lower bound for the exponential integral given in Lemma 1. Using this lower bound, we obtain

$$\begin{aligned} & \mathbb{E}_{\xi_1} \left[\log_2 (b_1 + \alpha_1 \xi_1) \mid \xi_{2:K} \right] \\ &> \frac{1}{\ln(2)} \left(\ln(b_1) + \ln \left(1 + e^{-\gamma} \frac{2\alpha_1}{b_1} \right) \right) \\ &= \log_2 (b_1 + 2e^{-\gamma} \alpha_1) \end{aligned} \quad (71)$$

where γ is the Euler-Mascheroni constant. By defining

$$b_k = 2e^{-\gamma} \sum_{j=1}^{k-1} \alpha_j + \sum_{j=k+1}^K \alpha_j \xi_j \quad (72)$$

and by iteratively proceeding with the same method for $k = 2, \dots, K$ as we did above for $k = 1$, we have in the k -th step

$$\begin{aligned} & \mathbb{E}_{\xi_{k:K}} \left[\log_2 (b_{k-1} + 2e^{-\gamma} \alpha_{k-1}) \right] \\ &= \mathbb{E}_{\xi_{k:K}} \left[\log_2 (b_k + \xi_k \alpha_k) \right] \\ &= \mathbb{E}_{\xi_{k+1:K}} \left[\mathbb{E}_{\xi_k} \left[\log_2 (b_k + \alpha_k \xi_k) \mid \xi_{k+1:K} \right] \right] \\ &> \mathbb{E}_{\xi_{k+1:K}} \left[\log_2 (b_k + 2e^{-\gamma} \alpha_k) \right]. \end{aligned} \quad (73)$$

Hence, iteratively applying the bound in (71) for all $k = 1, \dots, K$, we obtain in the final K th step the value $b_K = 2e^{-\gamma} \sum_{k=1}^{K-1} \alpha_k$ and, therefore, we can bound the expression in (68) as

$$\mathbb{E}_{\xi_{1:K}} \left[\log_2 \left(\sum_{k=1}^K \alpha_k \xi_k \right) \right] > \log_2 \left(2e^{-\gamma} \sum_{k=1}^K \alpha_k \right). \quad (74)$$

This bound is valid for $K \geq 2$. When $K = 1$ the situation is different and we can directly obtain an expression for the expression in (67), given by

$$\mathbb{E}[\text{Mit}] \geq \mathbb{E}_{\boldsymbol{\theta}} \left[\mathbb{E}_{\xi_1} \left[\log_2 (\alpha_1 \xi_1) \right] \right] = \mathbb{E}_{\boldsymbol{\theta}} \left[\log_2 (\alpha_1) + \mathbb{E}_{\xi_1} \left[\log_2 (\xi_1) \right] \right]. \quad (75)$$

From [45, p. 943, eq. (26.4.36)], we know that

$$\mathbb{E}_{\xi_1} \left[\log_2 (\xi_1) \right] = \log_2(2) + \mathbb{E}_{\xi_1} \left[\log_2 \left(\frac{\xi_1}{2} \right) \right] = \log_2(2) + \psi(1) \quad (76)$$

where $\psi(\bullet)$ is the digamma function. Using [45, p.258, eq. (6.3.2)], we have $\psi(1) = -\gamma$ and, hence, we arrive at

$$\mathbb{E}_{\xi_1} \left[\log_2 (\alpha_1 \xi_1) \right] = \log_2(2e^{-\gamma} \alpha_1). \quad (77)$$

Combining the bound from (74) for $K \geq 2$ and the expression for $K = 1$ in (77), we obtain the bound for equation (63) with the help of (67) as

$$\begin{aligned} \mathbb{E}[\text{Mit}] &\geq \mathbb{E}_{\mathbf{h}_{r,K+1}, \boldsymbol{\theta}} \left[\mathbb{E}_{\mathbf{H}_r^\dagger | \mathbf{h}_{r,K+1}, \boldsymbol{\theta}} \left[\log_2 \left(\sum_{k=1}^K \frac{|h_k|^2}{\operatorname{tr}(\mathbf{R}_{d,k})} \right) \right] \right] \\ &= \mathbb{E}_{\mathbf{h}_{r,K+1}, \boldsymbol{\theta}} \left[\mathbb{E}_{\mathbf{H}_r^\dagger | \mathbf{h}_{r,K+1}, \boldsymbol{\theta}} \left[\log_2 \left(\sum_{k=1}^K \alpha_k \xi_k \right) \right] \right] \\ &\geq \mathbb{E}_{\mathbf{h}_{r,K+1}, \boldsymbol{\theta}} \left[\log_2 \left(2e^{-\gamma} \sum_{k=1}^K \alpha_k \right) \right] \\ &= \mathbb{E}_{\mathbf{h}_{r,K+1}, \boldsymbol{\theta}} \left[\log_2 \left(e^{-\gamma} \sum_{k=1}^K \frac{\boldsymbol{\theta}^H \mathbf{R}_{c,k} \boldsymbol{\theta}}{\operatorname{tr}(\mathbf{R}_{d,k})} \right) \right] \end{aligned} \quad (78)$$

and the final upper bound of the ergodic rate is given by

$$\mathbb{E}[\overline{\text{SE}}_{\text{Lin},r}] \leq \mathbb{E} \left[\log_2 \left(\frac{|\mathbf{h}_{c,K+1}^H \boldsymbol{\theta}|^2 \bar{p}}{e^{-\gamma} \sum_{k=1}^K \frac{\boldsymbol{\theta}^H \mathbf{R}_{c,k} \boldsymbol{\theta}}{\operatorname{tr}(\mathbf{R}_{d,k})}} \right) \right]. \quad (79)$$

E. SE Expressions for Random/Statistical Phase Shifts under i.i.d. Rayleigh Fading

Under Rayleigh fading, it is possible to derive an exact expression for

$$\mathbb{E} \left[\log_2 \left(|\mathbf{h}_{c,K+1}^H \boldsymbol{\theta}|^2 \bar{p} \right) \right]. \quad (80)$$

We start similar to Appendix D by defining

$$\xi = \frac{2}{\text{var}[\mathbf{h}_{c,K+1}^H \boldsymbol{\theta}]} |\mathbf{h}_{c,K+1}^H \boldsymbol{\theta}|^2 \sim \chi^2(2) \quad (81)$$

which is chi-squared distributed with two degrees of freedom and the variance $\text{var}[\mathbf{h}_{c,K+1}^H \boldsymbol{\theta}]$ is given by

$$\text{var}[\mathbf{h}_{c,K+1}^H \boldsymbol{\theta}] = \mathbb{E}[|\mathbf{h}_{c,K+1}^H \boldsymbol{\theta}|^2] = \boldsymbol{\theta}^H \mathbf{R}_{c,K+1} \boldsymbol{\theta}. \quad (82)$$

Using (77) according to [45, p. 258, eq. (6.3.2)], we have

$$\begin{aligned} \mathbb{E}[\log_2(|\mathbf{h}_{c,K+1}^H \boldsymbol{\theta}|^2 \bar{p})] &= \mathbb{E}\left[\log_2\left(\frac{1}{2} \boldsymbol{\theta}^H \mathbf{R}_{c,K+1} \boldsymbol{\theta} \xi \bar{p}\right)\right] \\ &= \log_2(e^{-\gamma} \boldsymbol{\theta}^H \mathbf{R}_{c,K+1} \boldsymbol{\theta} \bar{p}) \end{aligned} \quad (83)$$

for statistical/random phase shifts. Under i.i.d. Rayleigh fading, this reduces to

$$\mathbb{E}[\log_2(|\mathbf{h}_{c,K+1}^H \boldsymbol{\theta}|^2 \bar{p})] = \log_2(e^{-\gamma} L_{r,K+1} L_G N_B N_R \bar{p}) \quad (84)$$

and we arrive at the SE for DPC

$$\mathbb{E}[\overline{\text{SE}}_{\text{DPC},r}] = \log_2(e^{-\gamma} L_{r,K+1} L_G N_B N_R \bar{p}).$$

as well as the upper bound for linear precoding

$$\begin{aligned} \mathbb{E}[\overline{\text{SE}}_{\text{Lin},r}] &\leq \log_2\left(\frac{e^{-\gamma} L_{r,K+1} L_G N_B N_R \bar{p}}{e^{-\gamma} \frac{N_R L_G N_B}{N_B} \sum_{k=1}^K \frac{L_{r,k}}{L_{d,k}}}\right) \\ &= \log_2\left(N_B \frac{L_{r,K+1} \bar{p}}{\sum_{k=1}^K \frac{L_{r,k}}{L_{d,k}}}\right). \end{aligned} \quad (85)$$

F. Linear Precoding Upper Bound for Weak User Maximization under i.i.d. Rayleigh Fading

When considering the phases based on optimizing the weak user, i.e.,

$$\boldsymbol{\theta} = \exp(j \arg(\mathbf{h}_{c,K+1})) \quad (86)$$

we arrive at

$$\begin{aligned} \mathbb{E}[\log_2(|\mathbf{h}_{c,K+1}^H \boldsymbol{\theta}|^2 \bar{p})] &\leq \log_2\left(\mathbb{E}[|\mathbf{h}_{c,K+1}^H \boldsymbol{\theta}|^2] \bar{p}\right) \\ &= \log_2\left(\frac{\pi}{4} N_B L_G L_{r,K+1} N_R^2 \bar{p}\right) \end{aligned} \quad (87)$$

according to [49]. Hence, the upper bound in case of optimizing the weak user results in

$$\mathbb{E}[\overline{\text{SE}}_{\text{Lin},r}] \leq \log_2\left(\frac{\pi e^{\gamma}}{4} N_R N_B \frac{L_{r,K+1} \bar{p}}{\sum_{k=1}^K \frac{L_{r,k}}{L_{d,k}}}\right). \quad (88)$$

G. DPC Lower Bound for Weak User Maximization under i.i.d. Rayleigh Fading

We are considering i.i.d. Rayleigh Fading, i.e. $\mathbf{h}_{r,K+1} \sim \mathcal{N}_C(\mathbf{0}, \mathbf{I} L_{r,K+1})$ as well as the optimal phase shifts based on instantaneous CSI given by alignment as

$$\boldsymbol{\theta} = \exp(j \arg(\mathbf{h}_{c,K+1})). \quad (89)$$

In this case, we have

$$\mathbb{E}[\overline{\text{SE}}_{\text{DPC},r}] = \mathbb{E}\left[\log_2(|\mathbf{h}_{c,K+1}^H \boldsymbol{\theta}|^2 \bar{p})\right]$$

$$= \log_2(\bar{p}) + 2\mathbb{E}\left[\log_2\left(\sum_{n=1}^{N_R} |h_{c,K+1,n}|\right)\right]. \quad (90)$$

Defining

$$\zeta_n = \sqrt{\frac{2}{N_B L_{r,K+1} L_G}} |h_{r,K+1,n}|, \quad (91)$$

we obtain with Jensen's inequality

$$\begin{aligned} \mathbb{E}[\overline{\text{SE}}_{\text{DPC},r}] &= \log_2(\bar{p}) + 2\mathbb{E}\left[\log_2\left(\sqrt{\frac{N_B L_{r,K+1} L_G}{2}} \sum_{n=1}^{N_R} \zeta_n\right)\right] \\ &= \log_2\left(\frac{1}{2} N_B L_{r,K+1} L_G \bar{p} N_R^2\right) + 2\mathbb{E}\left[\log_2\left(\frac{1}{N_R} \sum_{n=1}^{N_R} \zeta_n\right)\right] \\ &\geq \log_2\left(\frac{1}{2} L'_G \bar{p} N_B N_R^2 L_{r,K+1}\right) + \frac{2}{N_R} \mathbb{E}\left[\sum_{n=1}^{N_R} \log_2(\zeta_n)\right]. \end{aligned} \quad (92)$$

By recognizing that ζ_n^2 is again chi-squared distributed with two degrees of freedom, we can use the same argumentation as in Eqn. (77) based on [45, p. 258, eq. (6.3.2)], after which we arrive at

$$\mathbb{E}[\log_2(\zeta_n)] = \frac{1}{2} \mathbb{E}[\log_2(\zeta_n^2)] = \frac{1}{2} \log_2(2e^{-\gamma}) \quad (93)$$

and obtain the lower bound

$$\mathbb{E}[\overline{\text{SE}}_{\text{DPC},r}] \geq \log_2(e^{-\gamma} L'_G L_{r,K+1} \bar{p} N_B N_R^2) \quad (94)$$

for the optimal phase shifts with instantaneous CSI under i.i.d. Rayleigh fading.

REFERENCES

- [1] Q. Wu and R. Zhang, "Intelligent Reflecting Surface Enhanced Wireless Network via Joint Active and Passive Beamforming," *IEEE Transactions on Wireless Communications*, vol. 18, no. 11, pp. 5394–5409, 2019.
- [2] J. Xu, Y. Liu, X. Mu, and O. A. Dobre, "STAR-RISs: Simultaneous Transmitting and Reflecting Reconfigurable Intelligent Surfaces," *IEEE Communications Letters*, vol. 25, no. 9, pp. 3134–3138, 2021.
- [3] Y. Liu, X. Mu, J. Xu, R. Schober, Y. Hao, H. V. Poor, and L. Hanzo, "STAR: Simultaneous Transmission and Reflection for 360° Coverage by Intelligent Surfaces," *IEEE Wireless Communications*, vol. 28, no. 6, pp. 102–109, 2021.
- [4] S. Shen, B. Clerckx, and R. Murch, "Modeling and Architecture Design of Reconfigurable Intelligent Surfaces Using Scattering Parameter Network Analysis," *IEEE Transactions on Wireless Communications*, vol. 21, no. 2, pp. 1229–1243, 2022.
- [5] H. Li, S. Shen, and B. Clerckx, "Beyond Diagonal Reconfigurable Intelligent Surfaces: From Transmitting and Reflecting Modes to Single-, Group-, and Fully-Connected Architectures," *IEEE Transactions on Wireless Communications*, vol. 22, no. 4, pp. 2311–2324, 2023.
- [6] Z. Zhang, L. Dai, X. Chen, C. Liu, F. Yang, R. Schober, and H. V. Poor, "Active RIS vs. Passive RIS: Which Will Prevail in 6G?" *IEEE Transactions on Communications*, vol. 71, no. 3, pp. 1707–1725, 2023.
- [7] C. You and R. Zhang, "Wireless Communication Aided by Intelligent Reflecting Surface: Active or Passive?" *IEEE Wireless Communications Letters*, vol. 10, no. 12, pp. 2659–2663, 2021.
- [8] C. Huang, A. Zappone, G. C. Alexandropoulos, M. Debbah, and C. Yuen, "Reconfigurable Intelligent Surfaces for Energy Efficiency in Wireless Communication," *IEEE Transactions on Wireless Communications*, vol. 18, no. 8, pp. 4157–4170, 2019.
- [9] H. Guo, Y.-C. Liang, J. Chen, and E. G. Larsson, "Weighted Sum-Rate Maximization for Reconfigurable Intelligent Surface Aided Wireless Networks," *IEEE Transactions on Wireless Communications*, vol. 19, no. 5, pp. 3064–3076, 2020.
- [10] C. Pan, H. Ren, K. Wang, W. Xu, M. El-kashlan, A. Nallanathan, and L. Hanzo, "Multicell MIMO Communications Relying on Intelligent Reflecting Surfaces," *IEEE Transactions on Wireless Communications*, vol. 19, no. 8, pp. 5218–5233, 2020.

- [11] S. Zhang and R. Zhang, "Capacity Characterization for Intelligent Reflecting Surface Aided MIMO Communication," *IEEE Journal on Selected Areas in Communications*, vol. 38, no. 8, pp. 1823–1838, 2020.
- [12] Y. Han, W. Tang, S. Jin, C.-K. Wen, and X. Ma, "Large Intelligent Surface-Assisted Wireless Communication Exploiting Statistical CSI," *IEEE Transactions on Vehicular Technology*, vol. 68, no. 8, pp. 8238–8242, 2019.
- [13] G. Gradoni and M. Di Renzo, "End-to-End Mutual Coupling Aware Communication Model for Reconfigurable Intelligent Surfaces: An Electromagnetic-Compliant Approach Based on Mutual Impedances," *IEEE Wireless Communications Letters*, vol. 10, no. 5, pp. 938–942, 2021.
- [14] J. A. Nossek, D. Semmler, M. Joham, and W. Utschick, "Physically Consistent Modelling of Wireless Links with Reconfigurable Intelligent Surfaces Using Multiport Network Analysis," 2023. [Online]. Available: <https://arxiv.org/abs/2308.12223>
- [15] A. Abrardo, A. Toccafondi, and M. D. Renzo, "Design of Reconfigurable Intelligent Surfaces by Using S-Parameter Multiport Network Theory – Optimization and Full-Wave Validation," 2023.
- [16] M. Nerini, S. Shen, H. Li, M. D. Renzo, and B. Clerckx, "A Universal Framework for Multiport Network Analysis of Reconfigurable Intelligent Surfaces," 2023.
- [17] J. A. Nossek, D. Semmler, M. Joham, and W. Utschick, "Modelling of Wireless Links with Reconfigurable Intelligent Surfaces Using Multiport Network Analysis," in *2024 27th International Workshop on Smart Antennas (WSA)*, 2024, pp. 1–8.
- [18] X. Qian and M. D. Renzo, "Mutual Coupling and Unit Cell Aware Optimization for Reconfigurable Intelligent Surfaces," *IEEE Wireless Communications Letters*, vol. 10, no. 6, pp. 1183–1187, 2021.
- [19] D. Semmler, J. A. Nossek, M. Joham, and W. Utschick, "Performance Analysis of Systems with Coupled and Decoupled RISs," 2024. [Online]. Available: <https://arxiv.org/abs/2402.15423>
- [20] A. L. Swindlehurst, G. Zhou, R. Liu, C. Pan, and M. Li, "Channel Estimation With Reconfigurable Intelligent Surfaces—A General Framework," *Proceedings of the IEEE*, vol. 110, no. 9, pp. 1312–1338, 2022.
- [21] M. Joham, H. Gao, and W. Utschick, "Estimation Of Channels In Systems With Intelligent Reflecting Surfaces," in *ICASSP 2022 - 2022 IEEE International Conference on Acoustics, Speech and Signal Processing (ICASSP)*, 2022, pp. 5368–5372.
- [22] B. Fesl, A. Faika, N. Turan, M. Joham, and W. Utschick, "Channel Estimation with Reduced Phase Allocations in RIS-Aided Systems," in *2023 IEEE 24th International Workshop on Signal Processing Advances in Wireless Communications (SPAWC)*, 2023, pp. 161–165.
- [23] Z. Peng, C. Pan, G. Zhou, H. Ren, S. Jin, P. Popovski, R. Schober, and X. You, "Two-Stage Channel Estimation for RIS-Aided Multiuser mmWave Systems With Reduced Error Propagation and Pilot Overhead," *IEEE Transactions on Signal Processing*, vol. 71, pp. 3607–3622, 2023.
- [24] M.-M. Zhao, Q. Wu, M.-J. Zhao, and R. Zhang, "Intelligent Reflecting Surface Enhanced Wireless Networks: Two-Timescale Beamforming Optimization," *IEEE Transactions on Wireless Communications*, vol. 20, no. 1, pp. 2–17, 2021.
- [25] K. Zhi, C. Pan, H. Ren, and K. Wang, "Power Scaling Law Analysis and Phase Shift Optimization of RIS-Aided Massive MIMO Systems With Statistical CSI," *IEEE Transactions on Communications*, vol. 70, no. 5, pp. 3558–3574, 2022.
- [26] S. Syed, D. Semmler, D. B. Amor, M. Joham, and W. Utschick, "Design of a Single-User RIS-Aided MISO System Based on Statistical Channel Knowledge," in *2023 57th Asilomar Conference on Signals, Systems, and Computers*, 2023, pp. 460–464.
- [27] M. Costa, "Writing on Dirty Paper (corresp.)," *IEEE Transactions on Information Theory*, vol. 29, no. 3, pp. 439–441, 1983.
- [28] H. Weingarten, Y. Steinberg, and S. Shamai, "The Capacity Region of the Gaussian Multiple-Input Multiple-Output Broadcast Channel," *IEEE Transactions on Information Theory*, vol. 52, no. 9, pp. 3936–3964, 2006.
- [29] J. Lee and N. Jindal, "High SNR Analysis for MIMO Broadcast Channels: Dirty Paper Coding Versus Linear Precoding," *IEEE Transactions on Information Theory*, vol. 53, no. 12, pp. 4787–4792, 2007.
- [30] R. Hunger and M. Joham, "An asymptotic analysis of the MIMO broadcast channel under linear filtering," in *2009 43rd Annual Conference on Information Sciences and Systems*, 2009, pp. 494–499.
- [31] Q. Wu and R. Zhang, "Towards Smart and Reconfigurable Environment: Intelligent Reflecting Surface Aided Wireless Network," *IEEE Communications Magazine*, vol. 58, no. 1, pp. 106–112, 2020.
- [32] Q.-U.-A. Nadeem, A. Kammoun, A. Chaaban, M. Debbah, and M.-S. Alouini, "Asymptotic Max-Min SINR Analysis of Reconfigurable Intelligent Surface Assisted MISO Systems," *IEEE Transactions on Wireless Communications*, vol. 19, no. 12, pp. 7748–7764, 2020.
- [33] E. Björnson and P. Ramezani, "Maximum Likelihood Channel Estimation for RIS-Aided Communications with LOS Channels," in *2022 56th Asilomar Conference on Signals, Systems, and Computers*, 2022, pp. 403–407.
- [34] A. Papazafeiropoulos, P. Kourtessis, K. Ntontin, and S. Chatzinotas, "Joint Spatial Division and Multiplexing for FDD in Intelligent Reflecting Surface-Assisted Massive MIMO Systems," *IEEE Transactions on Vehicular Technology*, vol. 71, no. 10, pp. 10754–10769, 2022.
- [35] Q.-U.-A. Nadeem, H. Alwazani, A. Kammoun, A. Chaaban, M. Debbah, and M.-S. Alouini, "Intelligent Reflecting Surface-Assisted Multi-User MISO Communication: Channel Estimation and Beamforming Design," *IEEE Open Journal of the Communications Society*, vol. 1, pp. 661–680, 2020.
- [36] Q. Wu and R. Zhang, "Intelligent Reflecting Surface Enhanced Wireless Network: Joint Active and Passive Beamforming Design," in *2018 IEEE Global Communications Conference (GLOBECOM)*, 2018, pp. 1–6.
- [37] D. Semmler, M. Joham, and W. Utschick, "High SNR Analysis of RIS-Aided MIMO Broadcast Channels," in *2023 IEEE 24th International Workshop on Signal Processing Advances in Wireless Communications (SPAWC)*, 2023, pp. 221–225.
- [38] —, "A Zero-Forcing Approach for the RIS-Aided MIMO Broadcast Channel," *arXiv*, <https://arxiv.org/pdf/2311.11769.pdf>, 2023.
- [39] Ö. Özdogan, E. Björnson, and E. G. Larsson, "Using Intelligent Reflecting Surfaces for Rank Improvement in MIMO Communications," in *2020 IEEE International Conference on Acoustics, Speech and Signal Processing (ICASSP)*, 2020, pp. 9160–9164.
- [40] E. Björnson, Ö. Özdogan, and E. G. Larsson, "Intelligent Reflecting Surface Versus Decode-and-Forward: How Large Surfaces are Needed to Beat Relaying?" *IEEE Wireless Communications Letters*, vol. 9, no. 2, pp. 244–248, 2020.
- [41] X. Yu, D. Xu, and R. Schober, "Enabling Secure Wireless Communications via Intelligent Reflecting Surfaces," in *2019 IEEE Global Communications Conference (GLOBECOM)*, 2019, pp. 1–6.
- [42] D. Semmler, M. Joham, and W. Utschick, "Linear Precoding in the Intelligent Reflecting Surface Assisted MIMO Broadcast Channel," in *2022 IEEE 23rd International Workshop on Signal Processing Advances in Wireless Communication (SPAWC)*, Oulu, Finland, Jul. 2022.
- [43] N. S. Perović, L.-N. Tran, M. D. Renzo, and M. F. Flanagan, "On the Maximum Achievable Sum-Rate of the RIS-Aided MIMO Broadcast Channel," *IEEE Transactions on Signal Processing*, vol. 70, pp. 6316–6331, 2022.
- [44] C. Guthy, W. Utschick, R. Hunger, and M. Joham, "Efficient Weighted Sum Rate Maximization With Linear Precoding," *IEEE Transactions on Signal Processing*, vol. 58, no. 4, pp. 2284–2297, 2010.
- [45] M. Abramowitz and I. A. Stegun, Eds., *Handbook of Mathematical Functions with Formulas, Graphs and Mathematical Tables*. New York: Dover Publications, Inc., 1965.
- [46] W. Gautschi, "Some Elementary Inequalities Relating to the Gamma and Incomplete Gamma Function," *Journal of Mathematics and Physics*, vol. 38, pp. 77–81, 1959. [Online]. Available: <https://api.semanticscholar.org/CorpusID:124100683>
- [47] H. Alzer, "On Some Inequalities for the Incomplete Gamma Function," *Mathematics of Computation*, vol. 66, no. 218, pp. 771–778, 1997. [Online]. Available: <http://www.jstor.org/stable/2153894>
- [48] K. Nantomah, "On Some Bounds for the Exponential Integral Function," *Journal of Nepal Mathematical Society*, vol. 4, pp. 28–34, 12 2021.
- [49] I. Singh, P. J. Smith, and P. A. Dmochowski, "Optimal SNR Analysis for Single-user RIS Systems," in *2021 IEEE 32nd Annual International Symposium on Personal, Indoor and Mobile Radio Communications (PIMRC)*, 2021, pp. 549–554.